Influence of Temperature and Water content of Soil on Electrical Resistivity Tomography (ERT)

Omoghomion Oredia

School of Engineering

Thesis submitted for examination for the degree of Master of Science in Technology.

Espoo 11.02.2020

Supervisor

Prof. Jussi Leveinen

Advisor

PhD. Tero Hokkanen

Aalto University
School of Engineering

Aalto University
School of Engineering

Aalto University, P.O. BOX 11000, 00076 AALTO
www.aalto.fi
Abstract of the master's thesis

Author Omoghomion Oredia

Title Influence of Temperature and Water content of Soil on Electrical Resistivity Tomography (ERT)

Degree programme Geoengineering

Major Geoengineering **Code of major** ENG23

Supervisor Prof. Jussi Leveinen

Advisor PhD. Tero Hokkanen

Date 11.02.2020 **Number of pages** 73+7 **Language** English

Abstract

Soil is a dynamic natural body having different properties determined by its origin, modified over time by several geological deformations like glacial rebounds. Several geological and geotechnical techniques have been developed over the years to investigate this dynamic nature of the soil. One of the essential means to study the properties of soils is the Electrical Resistivity Tomography (ERT), which is a non-destructive and inexpensive method of investigation. Although the ERT method provides accurate information on the soil resistivity, the accuracy of the result obtained is however influenced for instance by temperature and water content of the soil. It is common knowledge that the resistivity of soil is affected by its water content and temperature. However, the temperature effect is neglected very often in some ERT studies. Therefore, this thesis concentrates particularly on the effects of the temperature but also water content of the soil on the soil resistivity.

This study involves onsite measurements of soil resistivity while monitoring and measuring the soil water content, temperature, and conductivity at different intervals by TDR probe buried beneath the soil surface. Finally, the resistivity of the soil samples obtained from different locations around Metsähovi and Aalto University, Otaniemi campus are measured under controlled laboratory conditions by varying the soil water content and temperature.

The results obtained in both cases show that the soil resistivity decrease with an increase in soil moisture. However, it seems that the temperature effect on ERT values is higher with lower soil water content and possibly the soil particle size and texture.

Keywords Electric resistivity tomography (ERT), Water content, Temperature, Resistivity, Soil

Preface

This thesis is inspired from my passion to to show the relevance of Geophysics as a remote sensing tool in engineering works.

First of all, I want to thank my supervisor Professor Jussi Leveinen for his whole-hearted attitude and advice throughout my thesis project and studies. Special thanks to my instructor Tero Hokkanen, the Senior Geophysicist and owner of GeoBlast Finland for offering a comprehensive background of this study and supporting me in carrying it out.

I would like to express my sincere gratitude to the Aalto laboratory technicians from the Civil engineering department, for providing me with the required equipment and important knowledge to carry out the tests for this thesis.

Additionally, I would like to thank my friends Osaruyi Osemwinyen, Ibrahima Kalil Fofana, Oluwabunmi Michael Agbede, Paul Kengne, as well as my girlfriend Ubi Iwali for their huge source of motivation throughout my thesis project and studies.

Finally, I wish to thank my family for supporting me during my entire studies.

Otaniemi, 11.02.2020

Omoghomion Oredia

Contents

List of Figures

List of Tables

Symbols and abbreviations

Symbols

$\propto$	Proportionality
$\frac{\partial v}{\partial x}$	Potential gradient
∂v	Potential difference
∂r	Radius of equipotential surface
$\approx$	Approximately equal to
$\leq$	Greater than or equal to

Abbreviations

EC	Electrical conductivity
ERT	Electrical resistivity tomography
M.H	Metsähovi
O.T	Otaniemi
SAS	Signal Averaging System
T.T	Tietotie
VES	Vertical electrical sounding

1 Introduction

Electrical resistivity tomography (ERT) method for subsurface investigation is widely used to study various properties of rocks and soil. A typical ERT involves the measurement of the apparent resistivity of subsurface materials by injecting electric current in the subsurface through current electrodes and measuring the potential difference across the potential electrodes. The electrical conductivity (EC) of rocks and soil are highly dependent on water saturation and ionic concentration within the pore water (Haley et al., 2010). Commonly, when ERT measurement is done, the temperature of the subsurface material is not taken into account thereby affecting the accuracy of apparent resistivity result of the subsurface. Michot et.al, (2003) showed that the thermal profile of the soil during electrical resistivity measurements was taken into account in the calculation since temperature variations in the soil affect the electrical resistivity of the water and therefore that of the soil. Resistivity changes are related also to freezing and thawing processes (Hauck, 2002). This phenomenon is highly obtainable in Finland as the seasonal variation in groundwater level and the hydrological cycle is largely influenced by snow cover and soil frost. Okkonen (2001) has investigated that the prevailing climate conditions in different parts of Finland has resulted in groundwater level fluctuation with groundwater level usually at a depth of 2 to 4 m below the surface but this depth can vary up to 30 m in some regions of southern Finland. Green et al., (2011) have also studied on a global scale how temperature and precipitation due to climate change have influenced groundwater recharge and groundwater levels. This phenomenon over time may influence the ERT measurement data of a region considering that the water content of soils is directly influenced by precipitation and changes in groundwater level. Rein et. al., (2004) also studied how the EC of subsurface materials is affected by changing water content, groundwater temperature, and even variation in diurnal temperature.

In this study, data from six different soil samples were used in the analysis. Five of the soil samples were collected in the Otaniemi area with one field measurement done in the area. The sixth soil sample was collected from Metsähovi for laboratory ERT measurement, as well as field ERT data provided by Hokkanen (2011). The different soil samples obtained from the field for laboratory measurement was identified using geotechnical laboratory methods after which they are subjected to different temperature and water content conditions in a controlled environment to measure the effect on the soil resistivity values. This is done to replicate similar conditions obtained when ERT field survey is carried out.

1.1 Hypothesis

Since water content and temperature affect ERT data, this effect should be eliminated before the interpretation to avoid ambiguous results.

1.2 Thesis structure

The structure of this thesis work is as follows:

- Chapter 2 focuses on the literature review and describes how ERT measurements are done and the principles guiding the application of ERT as a non-destructive method for subsurface investigation.
- Chapter 3 provides geological information about the samples and the origin of the soil materials.
- Chapter 4 gives information on the characterization of the soil samples used for this research.
- Chapter 5 focuses on data collection on analytical methods. It provides detailed information on how the ERT measurement was done for the soil samples and the data collection.
- Chapter 6 is about the interpretation of the resistivity results from the ERT measurement and discussion of the result with significance to the correlation of laboratory results with field measurements.
- Chapter 7 gives the conclusion of the research work and also the answer to the research questions.
- Chapter 8 gives recommendations for further investigations.

1.3 Research questions

The research questions based on the hypotheses for this research has been highlighted as follows:

1. How soil temperature affects ERT measurements and hence engineering works in different geological settings.
2. How soil water content affects ERT measurements and hence engineering works in different geological settings.
3. What is the relationship between soil resistivity, soil water content and soil temperature on ERT measurements.

1.4 Objectives

The following objectives are set and addressed in this thesis to answer the questions posed by this research:

1. Explain the ERT measurement method and its importance to engineering works.

2. Obtain resistivity data from different soil types within a range of temperature and water content value.
3. Characterise the different soil samples using geotechnical laboratory measurements.
4. Relationship of soil resistivity with temperature changes.
5. Characterize resistivity behaviour of various soil types with changing temperature and water content.

1.5 Limitations

The scope of the thesis work is to use different soil types at varying water content and temperature while taking ERT measurements in the laboratory and the field. The idea is to implement proper soil conditions as it is obtainable on the field, but this is not likely to be the case as there are several conditions such as pore water pressure, soil matrix arrangement which cannot be replicated in the laboratory. Although this may be the case, it has some effect on the laboratory ERT measurement. The seasonal condition can also be a limitation in this work as it is difficult to make field ERT measurement and take soil samples when there is frost in the soil. In conditions where there is frost in the soil, longer electrodes are used and they are pushed deeper and kept in soil throughout the monitoring. This was not possible in Otaniemi since we had data only from summer time.

2 Literature review

This chapter will provide a brief scope of the theoretical background to electrical resistivity measurement, together with the electric resistivity of Earth materials and its temperature and water content dependency. It also reviews the ERT measuring system, the array types, and modes of deployment.

2.1 Electrical resistivity method

The electrical resistivity geophysical method uses an artificial source of current which is passed into the subsurface or soil through point electrodes called the current electrodes, while the difference in potential of the subsurface is measured by other electrodes in the proximity of the current flow. This approach makes the resistivity method theoretically superior to all other Electrical methods because quantitative results are obtained by using a controlled source of specific dimension (Telford et.al, 1990). The electrical resistivity method uses inexpensive geophysical equipment and is relatively easy to perform.

This geophysical method is widely used in engineering works to identify groundwater aquifers and to locate sub-surface cavities, faults and fissures, permafrost, mineshafts etc. Electric resistivity methods are nondestructive and more environmentally friendly in studies of contaminated soils compared to drilling investigations which are always associated with the risk of drilling into the waste and spreading contaminants. Also, resistivity surveying is widely used in the search for geothermal reservoirs and in groundwater exploration, which is of increasing importance in civil engineering and worldwide.

2.1.1 True and Apparent resistivity

The theory of the electrical resistivity method is based on a few very important equations in which Ohm's Law applies in the vast majority of geophysical cases (Reynolds 1997). Resistivity surveying involves measuring the potential difference between two current electrodes while the potential at each electrode is determined due to the current sources. According to Ohm's Law, the current that flows through a material is directly proportional to the applied voltage (V), where the constant of proportionality is the resistance (R) to the flow of current through the material. Georg Simon Ohm (1787–1854) first demonstrated experimentally how the current in a metal wire is directly proportional to the voltage applied, see Eq. (1).

$$I \propto V \tag{1}$$

$$R = \frac{V}{I} \tag{2}$$

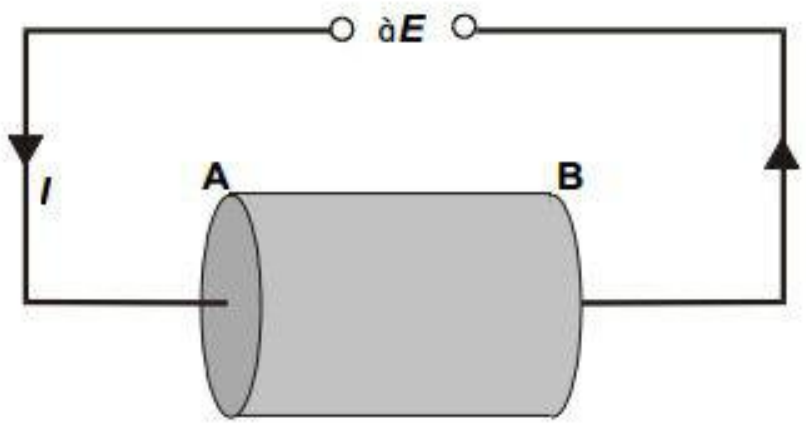

Figure 2.1: Ohm's Law for a rock sample.

The potential difference (∂E) between the ends of a cylindrical rock sample with two flat faces A and B of length L will have current (I) flow through the rock from face A to face B as shown in Figure (2.1). The resistance of the rock sample can be calculated using Eq. (2) if the current and the potential difference is measured. The value of the measured resistance R shows how much the material resists the passage of a current for a given applied potential difference is given by Eq. (3). From the Ohm's Law, the ratio of the potential drop to the applied current also defines the resistance of the cylindrical rock, hence the resistivity ρ can be defined by Eq. (4).

$$R = \frac{\rho L}{A} \tag{3}$$

where:

R = the measured resistance in ohms (Ω)

ρ = the resistivity of the sample in ohm-meter (Ωm)

L = length of the sample (m)

A = cross-sectional area of the sample perpendicular to the current flow (m^2)

Combining Eq. (2) and Eq. (3).

$$\rho = \frac{VA}{IL} \tag{4}$$

where:

ρ = the resistivity of the sample in ohm-meter (Ωm)

V = potential difference across the sample in volts (V)

A = cross-sectional area of the sample perpendicular to the current flow (m^2)

I = current flowing through the sample in amperes (A)

L = length of the sample (m).

This can also be expressed as conductivity C defined as the reciprocal of resistivity (R)

$$C = \frac{I}{R} = \frac{IL}{VA} \tag{5}$$

where:

C = conductivity of the sample in siemens per meter (S/m).

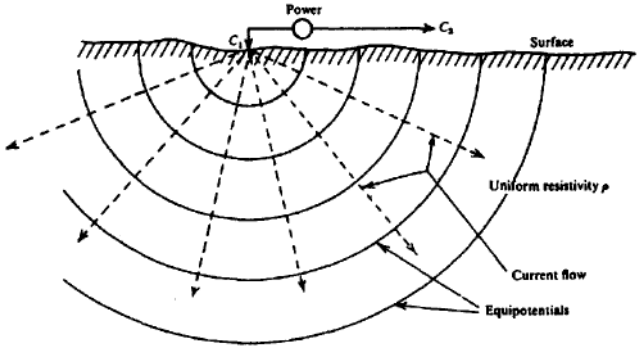

Figure 2.2: Point source of current at the surface of a homogeneous medium (Telford et.al, 1990).

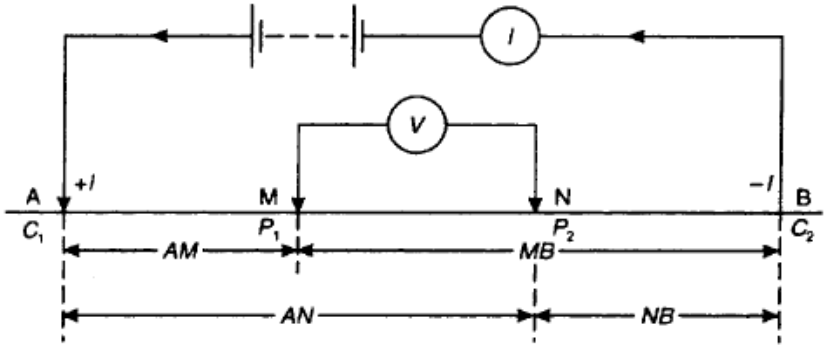

Figure 2.3: Generalised form of electrode configuration in resistivity surveys (Reynolds, 1997).

The measured electrical resistivity between the applied current and the potential difference for a specific configuration and spacing of electrodes, which corresponds to the sensitivity the subsurface would have if it were homogeneous is known as the apparent resistivity. The apparent resistivity is equal to the true resistivity as long as

the measurement is made over a homogeneous surface. However, when the resistance is made over a complicated subsurface structure, the apparent resistivity is a weighted average of the resistivities of the various rocks below the surface (McDowell et.al, 2002).

When current is injected into a homogenous medium of resistivity (ρ), the current flows radially through the medium which causes an equipotential surface, see Figure (2.2). The potential decreases in the direction of current flow and the voltage drop between any two points on the surface are known as the potential gradient, which is negative due to the potential decrease. The potential difference (∂v) of the equipotential surface of the radius (∂r) is given by;

$$\frac{\partial v}{\partial r} = -\frac{\rho I}{2\pi r^2} \tag{6}$$

$$V_r = \int \partial v = -\int \frac{I}{2\pi r^2}\partial v = \frac{\rho I}{2\pi}.\frac{1}{r} \tag{7}$$

by deduction the potential V_P at a point P is the sum of the potentials of the two current electrodes, such that $V_P = V_A + V_B$, see Figure (2.3). Hence, the potential at electrode M and N are:

$$V_M = \frac{\rho I}{2\pi}.[\frac{1}{AM} - \frac{1}{MB}] \tag{8}$$

$$V_N = \frac{\rho I}{2\pi}.[\frac{1}{AN} - \frac{1}{NB}] \tag{9}$$

Therefore, the potential difference between electrodes M and N is;

$$V_{MN} = V_M - V_N = \frac{\rho I}{2\pi}.\left\{[\frac{1}{AM} - \frac{1}{MB}] - [\frac{1}{AN} - \frac{1}{NB}]\right\} \tag{10}$$

$$\rho = \frac{2\pi V_{MN}}{I}.\left\{[\frac{1}{AM} - \frac{1}{MB}] - [\frac{1}{AN} - \frac{1}{NB}]\right\}^{-1} \tag{11}$$

In a non-uniform subsurface, Eq. (11) can be simplified as;

$$\rho = RK \tag{12}$$

K is known as the geometric factor and R the resistance.

$$K = 2\pi\left\{[\frac{1}{AM} - \frac{1}{MB}] - [\frac{1}{AN} - \frac{1}{NB}]\right\}^{-1} \tag{13}$$

$$R = \frac{\partial v}{I} \tag{14}$$

2.1.2 Electrical resistivity of Earth materials

Soils are composed of rock fragments or mineral particles, organic matter, water and air. Soil electrical resistivity is sensitive to its water content and dependent on its textural and structural characteristics (Michot et.al, 2003). The electrical resistivity of Earth materials (soils and rocks) has the widest range of variation of all the physical properties of earth materials (Telford et.al, 1990). There are different ways electric current transmits through earth materials. It could be by electronic conduction which takes place through materials such as metals, electrolytic conduction which is carried by ions in the pore water, and dielectric conduction which occurs by electrons and other charged particles in the presence of an electric field (Merritm, 2014). A good conductor is usually defined as a material of resistivity less than 10-5Ωm while an insulator is one having a resistivity greater than 107 Ωm and between this limit lies the semi-conductors (Telford et al., 1990). The common rocks and soils forming minerals have very high resistivity values when in a dry condition which means the resistivity of rocks and soils is a measure of the quantity of water in pores and fractures. The degree of connection between pore spaces is also important which consequently makes the resistivity of a rock type or soil type vary widely.

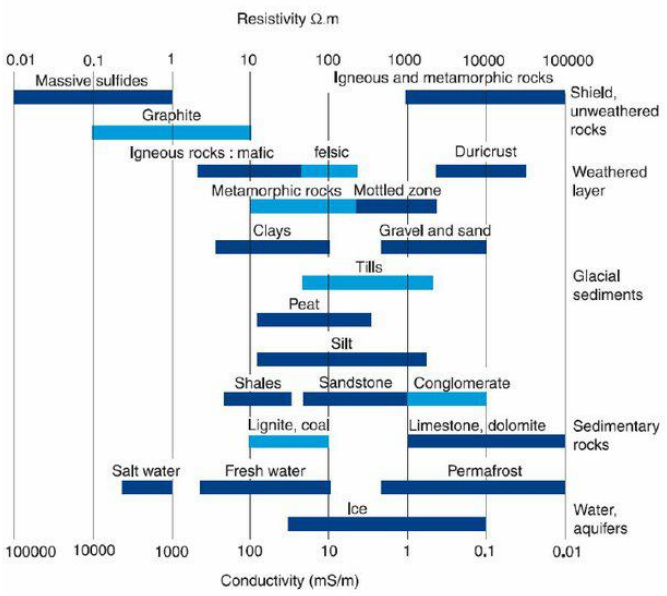

Figure 2.4: Resistivity of the main earth materials (Palacky, 1988).

Typical ranges of resistivities of geologic materials and different soil types are shown in Figure (2.4). The porosity of a material determines the amount of water it can take, and porosity is divided into primary porosity and secondary porosity. Primary porosity consists of pore spaces between the mineral particles and occurs in soils and sedimentary rocks. Secondary porosity consists of fractures and openings resulting from weathering or diagenetic processes, and this is the most important porosity in crystalline rocks such as granites and gneisses. Secondary porosity may also be important in certain sedimentary rocks such as limestone. Even if the porosity

is rather low, the electrical conduction taking place through water-filled pore spaces may reduce the resistivity of the material drastically. The degree of water saturation will affect the resistivity, thus the resistivity above the groundwater level will be higher than below if the material is the same. Archies law gives a relationship between porosity and the electrical property of saturated soil. This can be written as:

$$\rho = a\phi^{-m}S^{-n}\rho_w \tag{15}$$

where:

ρ = soil resistivity

ϕ = fractional pore volume (porosity)

S = fraction of pores containing water 7

ρ_w = resistivity of water

n $\approx$ 2, and a, m are constants, $0.5 \leq$ a ≤ 2.5, $1.3 \leq$ m ≤ 2.5.

Consequently, the method can be used to find the groundwater depth where a typical groundwater table exists. The resistivity of pore water is dominated by the type of ions, concentration of ions in solution, and the temperature. Clay minerals may be regarded as electrically conductive particles which can absorb and release ions and water molecules on its surface through an ion exchange process.

The dissolved ions concentration is usually measured as total dissolved solids (TDS). According to Corwin (2017), there is a correlation between electrical conductivity (EC) and total dissolved solids (TDS). The more salts dissolved in soil solution, the higher is the value of electrical conductivity in soil. A general relationship has often been applied to determine TDS from EC (Rusydi, 2018).

$$TDS(\frac{mg}{l}) = K \times EC(\frac{\mu S}{cm}) \tag{16}$$

where:

TDS = Total dissolved solids

K = Ratio of TDS/EC

EC = Electrical conductivity

However, a non directly linear relationship between EC and TDS excists which depends on the ionic strength of specific dissolved ions in the liquid. According to Rusydi (2018), the correlation ratio of TDS to EC in various types of freshwater are different, see Figure (2.5) and Figure (2.6). In Figure (2.5), TDS/EC ratio in freshwater(1) is 0.65 with correlation (R2 = 0.97).

$$TDS = 0.65 \times EC \tag{17}$$

While in Figure (2.6), TDS/EC ratio in freshwater(2) gives a higher TDS/EC ratio of 0.89 with similar correlation (R2 = 0.96).

$$TDS = 0.89 \times EC \tag{18}$$

Most common conversion factor (K) between EC and TDS are 0.55 and 0.75 but 0.65 is which is the average is used often. The 0.55 conversion factor is related to sodium chloride depends on EC and TDS while the 0.75 conversion factor is related to the mixture of sodium bicarbonate, sodium chloride, and sodium sulphate. TDS and EC relationship should be regarded as an empirical relationship, meaning the factor may vary from place to place due to variation in the composition of TDS.

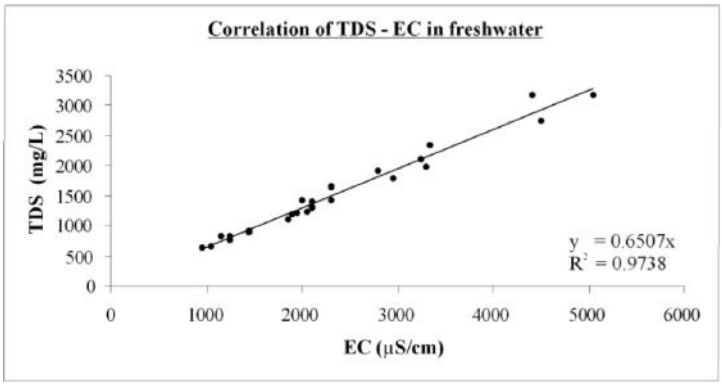

Figure 2.5: TDS – EC correlation in freshwater(1) (Rusydi, 2018).

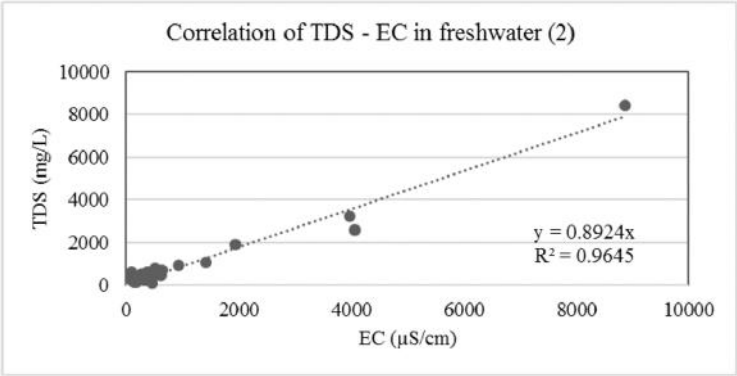

Figure 2.6: TDS – EC correlation in freshwater(2) (Rusydi, 2018).

The temperature influence is normally negligible due to the variation in ground temperature being small. However, the variation could be significant even in permafrost regions. As temperature increases the viscosity of water is lowered, hence the mobility of ions increases. this means a decrease in resistivity with increasing temperature can be observed for materials where electrolytic conduction dominates (Samouëlia et al., 2005). Campbell et al. (1948) studied the change of electrical conductivity with the temperature of different soils and showed that conductivity increase between 15°C and 35°C by 2.02 % per temperature degree celsius. This led

to the correction equation to express the electrical conductivity at the standardized temperature of 25°C. The equation is given as:

$$\rho_{25^\circ C} = \rho_t[1 + \alpha(T - 25^\circ C)] \tag{19}$$

where:

$\rho_{25^\circ C}$ = resistivity at 25°C

ρ_t = resistivity at the experiment temperature

α = correction factor equal to 2.02%

T = experiment temperature in °C

This equation relating soil temperature and conductivity are with accordance to the ISO/DIN7888 standard, and it has been discussed and used by several scholars like Samouëlia et al., (2005), Colman and Hendrix (1949), Michot et. Al., (2003) in research works related to electrical resistivity investigations. Schlumberger (1989) equation used to correct the temperature effect in the log interpretation chart corresponds to this equation hence verifying its validity.

Hu et al., (2019) have studied the effects of wetting-drying cycles on electrical resistivity and unconfined compressive strength of unsaturated compacted subgrade clay soil in the laboratory. For this study, three specimens at moisture content levels of 12%, 17%, and 22% were used to record the electrical resistivity at different temperatures. It shows that the electrical resistivity of the soil decreases with increasing moisture content and there is an almost linear relationship between the electrical resistivity of the Unsaturated Subgrade Soil and temperature, see Figure (2.7). Also, Bai et al. (2013) studied the effects of physical properties on the electrical conductivity of five compacted lateritic soil samples in the laboratory having dry densities (1.30 g/cm3, 1.38 g/cm3, 1.46 g/cm3, 1.54 g/cm3, and 1.58 g/cm3). The results from these studies showed that The electrical resistivity of the soil samples are notably influenced by water content, but this effect decreases when the water content is above 23.4%. This is close to the optimum water content, see Figure (2.8).

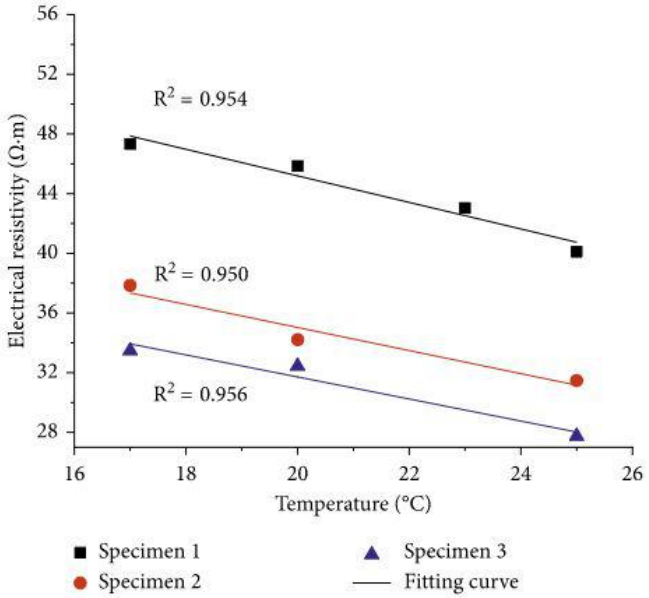

Figure 2.7: Relationship between electrical resistivity and temperature of different subgrade clay soil specimens (Hu et al., 2019).

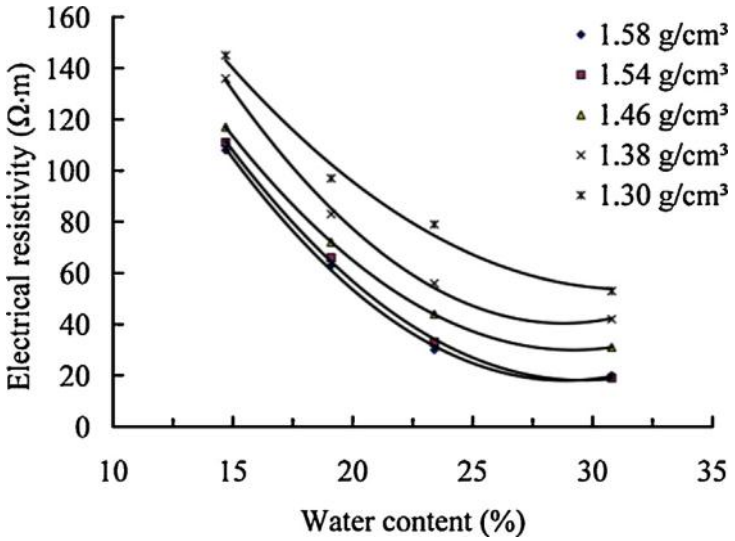

Figure 2.8: Relationship between water content and electrical resistivity of different compacted lateritic soil and their dry densities (Bai et al., 2013).

2.2 Electrical resistivity electrode configuration

The systematic and constant spacing of electrodes in resistivity surveys is known as electrical resistivity electrode configuration or array. Depending on the type of electrode configuration, the lateral and longitudinal changes in apparent resistivity of the subsurface reflecting geologic variability can be investigated (Reynolds, 1997). The apparent resistivity values measured in this resistivity survey is dependent

on the geometric factor (K), and the three main electrode configurations have different geometric factors. Two of these electrode configurations is named after their originators, Frank Wenner and Conrad Schlumberger. From these major configurations, several sub-arrays were developed to suit certain investigation purpose, shown in Table (2.1).

A generalized form of electrode configuration in resistivity surveys is shown in Figure (2.3). It consists of two current electrodes referred as A and B that are used to direct current into the subsurface, and two potential electrodes referred as M and N that are used to record the resulting potential difference. The potential difference ΔV measured between the electrodes M and N is given by Eq. (10), Where AM, MB, AN, and NB represents the geometrical distance between the electrodes A and M, B and M, A and N, and B and N, respectively. The electrical resistivity is then calculated using Eq. (11) where K from Eq. (13) is a geometrical coefficient or factor that depends on the arrangement of the four electrodes A, B, M and N.

To investigate changes in resistivity with depth, the size of the electrode array is varied with the spacing chosen to meet the need of the particular survey. This variation in electrode array gives rise to the different electrode configuration with each having its advantages and disadvantages (Reynolds, 1997). The choice of the array for an investigation is predominantly dependent on the sensitivity to both lateral and vertical inhomogeneities, the space available to set up the array, time and ease of deployment.

Table 2.1: Electrode configurations (Reynolds, 1997)

Wenner arrays	**Standard Wenner**
	Offset Wenner
	Lee-partitioning array
	Tripotential (α, β, and γ arrays)
Schlumberger array	**Standard schlumberger**
	Brant array
	Gradient array
Dipole-dipole arrays	**Normal** (axial or polar)
	Azimuthal
	Radial
	Parallel
	perpendicular
	Pole-Dipole
	Equatorial
	Square (special form of equatorial)

2.2.1 Wenner array

The Wenner array is the simplest and most widely used electrical resistivity configuration, with the electrodes uniformly spaced in a line. The Wenner array is useful

for resolving the differing resistivities of the subsurface layers straight down from the midpoint of the array (Herman, 2001). Since all the electrode spacing are equal as shown in Figure (2.9), then Eq. (13) becomes;

$$K = 2\pi a \tag{20}$$

Hence from Eq. (11) we have;

$$\rho_{Wenner} = (\frac{V_{MN}}{I})2\pi a \tag{21}$$

The simple geometric factor of the Wenner array makes it less complicated to execute and interpret data. For deep investigations, the electrode spacing is increased while maintaining the centre point. While for lateral investigation or mapping, the spacing is kept constant and all electrodes are moved along a line. The introduction of modern equipment which uses special algorithms to investigate the subsurface combines both vertically and laterally mapping. In this case, the electrode spacing is determined while the electrodes are placed in the subsurface with the appropriate spacing. The spacing distance is inputted in the resistivity meter which contains the special algorithm and measurement is taken. In this way, the electrodes are not moved physically but the algorithm does the selection of the electrodes while employing both the vertical and lateral Wenner profile form of measurements.

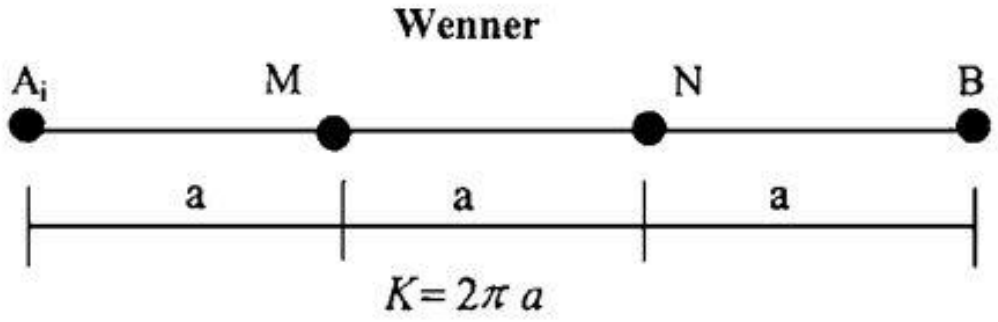

Figure 2.9: Schematic diagram of the Wenner array.

2.2.2 Schlumberger array

Schlumberger array, unlike the Wenner array, involves keeping the potential electrodes at fixed points M and N shown in Figure (2.10), and symmetrically increasing the current electrode separation A and B about the centre by moving the current electrodes outwardly in steps. This will increase the depth of penetration within the array separation line AB. Thus, the varying resistivity measured when the electrode array position is varied in an inhomogeneous medium is termed apparent resistivity. In the Schlumberger array, the current electrodes are spaced much further apart than the potential electrodes (Telford et.al, 1990).

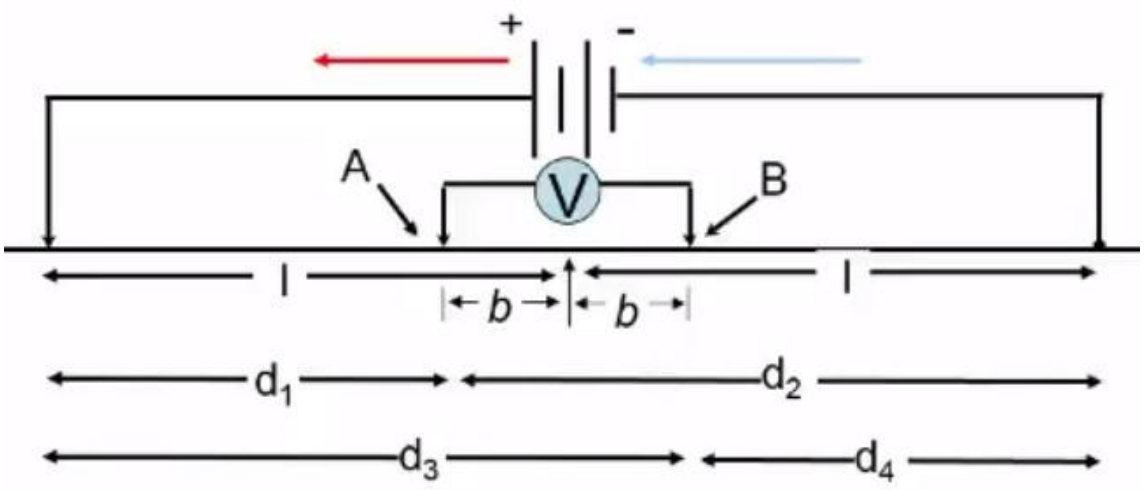

Figure 2.10: Schematic diagram of the Schlumberger array.

Compared to the Wenner array, the geometric factor of the Schlumberger array is more systematic in its derivation. From Figure (2.10), we have that;

d_1 = AM = l - b

d_2 = MB = l + b

d_3 = AN = l + b

d_4 = NB = l - b

Substituting these values in Eq.(13), we get

$$K = 2\pi \left\{ [\frac{1}{l-b} - \frac{1}{l+b}] - [\frac{1}{l+b} - \frac{1}{l-b}] \right\}^{-1} \tag{22}$$

$$K = 2\pi \left\{ [\frac{2}{l-b} - \frac{2}{l+b}] \right\}^{-1} \tag{23}$$

$$K = 2\pi \left\{ [\frac{2l+2b-2l+2b}{(l-b)(l+b)}] \right\}^{-1} \tag{24}$$

Which simplifies to;

$$K = 2\pi \left\{ [\frac{4b}{l^2-b^2}] \right\}^{-1} = 2\pi \frac{l^2-b^2}{4b} \tag{25}$$

$$K = \pi \frac{l^2-b^2}{2b} \tag{26}$$

This method is used often because it is faster and less likely to be influenced by lateral variations in the subsurface. It also requires a lower number of operators than the other methods as only the current electrodes A and B are displaced.

2.2.3 Dipole-dipole array

In the dipole-dipole electrode array two sets of electrodes, the current AB (source) and potential MN (receiver) electrodes are paired relatively close to one another. The convention for a dipole-dipole electrode array is to maintain an equal distance for both the current and the potential electrodes (spacing = a), with the distance between the current and potential electrodes as an integer multiple of the electrode spacing (a), see Figure (2.11). This electrode array is predominantly used where vertical penetration is paramount and its major drawback is the low vertical resolution obtained from its signal (Herman, 2001).

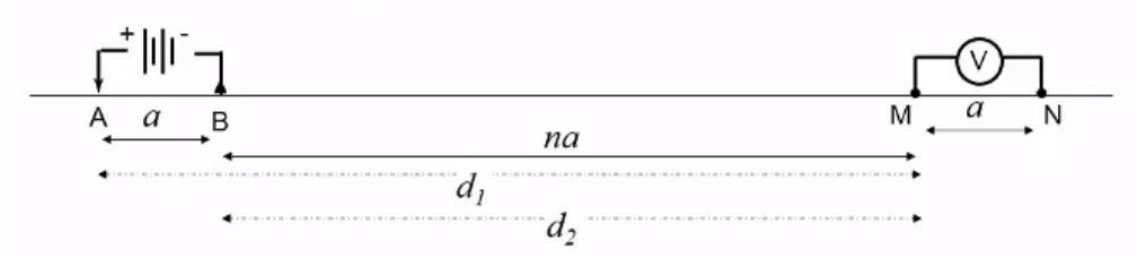

Figure 2.11: Schematic diagram of the Dipole dipole array.

From Figure (2.11), we have that;

d_1 = (n+1)a

d_2 = na

d_3 = (n+2)a

d_4 = (n+1)a

Substituting these values in Eq.(13), we get

$$K = 2\pi \left\{ [\frac{1}{(n+1)a} - \frac{1}{na}] - [\frac{1}{(n+2)a} - \frac{1}{(n+1)a}] \right\}^{-1} \tag{27}$$

$$K = 2\pi \left\{ [\frac{2}{(n+1)a} - \frac{1}{na} - \frac{1}{(n+2)a}] \right\}^{-1} \tag{28}$$

$$K = 2\pi \left\{ [\frac{a(n-1)}{na^2(n+1)} - \frac{1}{a(n+2)}] \right\}^{-1} \tag{29}$$

$$K = 2\pi \left\{ [\frac{a^2(n-1)(n+2) - na^2(n+1)}{na^3(n+1)(n+2)}] \right\}^{-1} \tag{30}$$

Which simplifies to;

$$K = 2\pi \left\{ [\frac{-2}{na(n+1)(n+2)}] \right\}^{-1} = -\pi na(n+1)(n+2) \tag{31}$$

All readings are taken as positive rather than minus, hence the minus sign is ignored.

$$K = -\pi na(n+1)(n+2) \tag{32}$$

2.3 Modes of electrical resistivity measurement

The mode of an electrical resistivity measurement depends on the purpose of the investigation. There are mainly two methods of deployment which are the vertical electrical sounding (VES) and lateral profiling. A third means of deployment technique known as electric imaging is used when both the VES and lateral profiling cannot give the desired results. With the introduction of modern types of equipment the electrical resistivity imaging method is mainly used.

2.3.1 Electrical resistivity imaging

Electrical resistivity imaging which is also known as electrical resistivity tomography (ERT) employs both VES and electrical resistivity profiling to investigate the subsurface by surveying both vertical and horizontal changes in resistivity. The idea is to increase electrode spacing while the survey profile is moved along a profile to measure both vertical and horizontal resistivity. With the use of Terrameter like the ABEM Terrameter SAS 1000 / SAS 4000, the electrodes are put in place while the equipment automatically sets the profile and selects the electrode in corresponding spacing. Imaging can be done in both 2D and 3D and the resistivity values got from the survey is used to create a pseudosection which can be used to generate an image of the subsurface, see Figure (2.12).

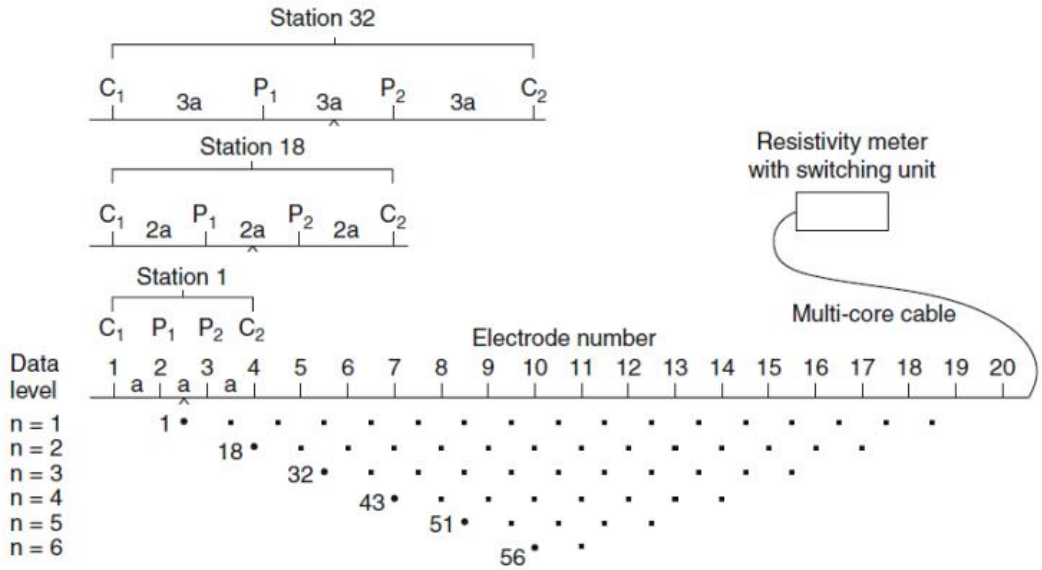

Figure 2.12: Sketch of the electrodes for 2D geoelectrical resistivity survey and the sequence of measurement for building a pseudosection (Loke, 2011).

2.4 Multiple-electrode electrical resistivity tomography measuring system

Electric resistivity measuring instruments range from very simple to highly sophisticated equipment with the latter including a computer for infield data processing. The essential parts of any resistivity instrumentation are a portable power source which is either D.C. or low-frequency A.C., stainless steel electrodes, cables and reels, and meters for measuring current and voltage both of which may be combined in a single meter reading resistance. With the development of computer-controlled data collection and also automatic data inversion, the use of computer-controlled multi-electrode systems with automatic data measurements and data quality control for the data acquisition allow a dramatic increase in in-field productivity.

The LUND Imaging System is a multi-electrode system for cost-effective and high-resolution 2D and 3D electrical resistivity surveys. It is an automatic electric imaging system suited for automatic resistivity profiling and sounding. The LUND Resistivity Imaging System consists of a basic unit, a standard resistivity meter (ABEM Terrameter SAS1000), and a multi-channel relay matrix switch unit called Electrode Selector ES 464. The system also has four multi-conductor electrode cables wound on reels each with 21 take-outs, stainless steel electrodes, cable jumpers, and various connectors. The system is compatible with a portable PC-type computer or notebook (laptop) used in data acquisition. This includes software featuring automatic measuring process, in-field quality control of measurements, automatic roll along, electrode cable geometry and switching sequence defined in address and protocol files which allow user-defined survey strategies and arrays, an onscreen echo of measurement progress, software for graphical and depth interpretation including pseudo section plotting in grayscale or colour. Model section plotting of 1D and 2D model interpretation sections in colour or grayscale including topography, reference data and reference levels, utility software for extraction of VES, data manipulation and conversion, graphical output in PCX-file format etc, are also available (ABEMLUND Instruction Manual). The Terrameter SAS system consists of a basic unit called the Terrameter SAS 1000 and accessories like ES 464. Signal Averaging System (SAS) is a method whereby consecutive readings are taken automatically and the results are averaged continuously. Signal Averaging System (SAS) results are more reliable than those obtained from single-short systems.

The SAS 4000 can operate in different modes like the resistivity, self-potential and induced polarization. The SAS 4000 is powered by a clip-on NiCd battery pack or by an external 12 volts source. The SAS-EBA external 12 volts adapter allows the Terrameter to utilize an external 12 volts D.C. source, e.g., a car battery (ABEMLUND Instruction Manual). Stainless steel electrodes establish electric contact between electronic conductors, which are long cables, to an ionic conductor which is the ground. Noise which is the fluctuating voltage that appears between a pair of electrodes placed so close usually occur at the potential electrodes. But with the use of stainless steel electrodes, less noise is created. Current electrodes and potential electrodes make good contact with the ground to ensure low contact resistance and stability respectively (ABEM Instrument AB, 2010). The cables

incorporate heavy gauge conductors with excellent insulation to ensure good survey results. The cables are expandable for deeper penetration by connecting them in series with a cable joint. The cables have takeouts at 5 meters intervals from which they are connected to the electrodes using cable jumpers having crocodile clips at both ends. The cables are wound on reels.

3 Location and Geology of the study area

The study area lies in the southern part of Finland along the coastal region of the Baltic sea. Both the resistivity field data and the six soil samples used to gather the laboratory resistivity data was gotten from Otaniemi and Metsähovi area. The Soil samples are named with the abbreviation of the location of extraction, see Figure (3.1).

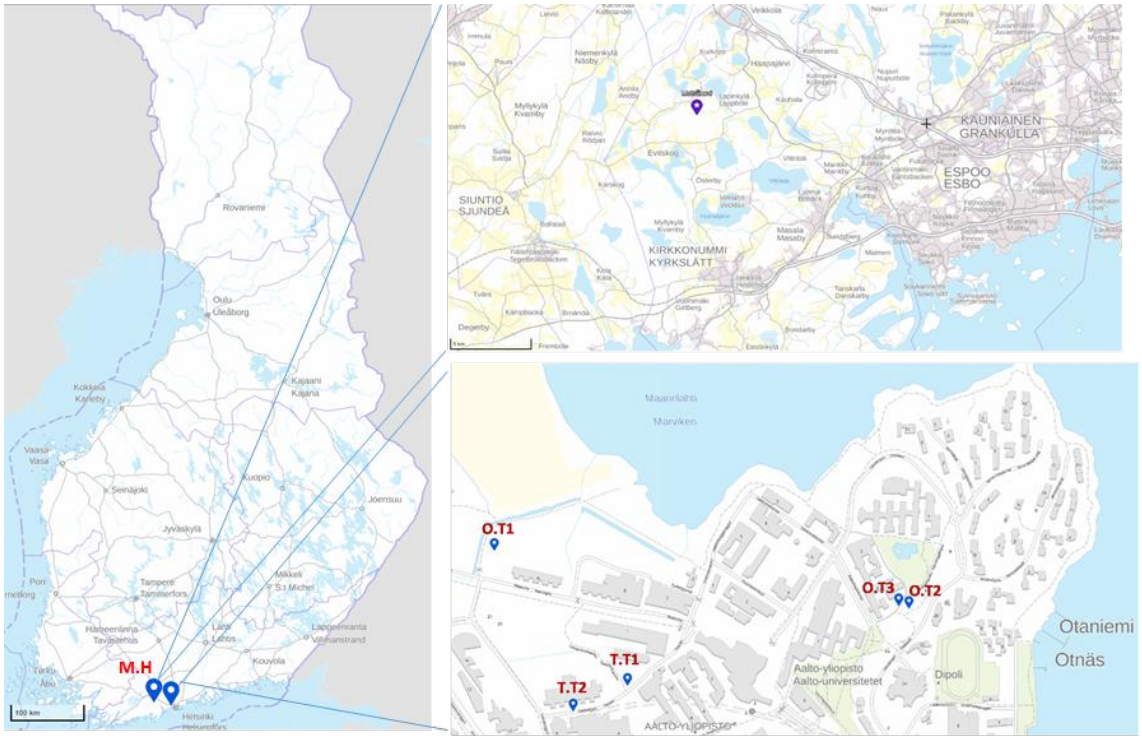

Figure 3.1: Background map showing the locations of the study area (Maanmittauslaitos).

The first sample (M.H) was extracted from the Metsähovi Geodetic Research Station which is located in Kirkkonummi, near Sjökulla in Southern Finland with 60m average elevation above sea level. The five other samples were extracted at specific locations at Aalto University in Otaniemi. T.T1 and T.T2 soil samples were collected along the Tietotie 1-lane road in the west side of Aalto University, Otaniemi campus. While O.T1 soil sample was collected approximately 500 meters north of T.T1 and T.T2. The soil samples for O.T2 and O.T3 was collected at the east side of Civil and Environmental Engineering building of Aalto University, Otaniemi campus.

Quaternary geology of Finland shows that glaciation has occurred four times during the Pleistocene time. This has left abraded bedrock and very thin average soil coverage in most places typically 6m and in some places 100m. Typically there are till layers as the lowermost soil layers above the bedrock at the bottom of soil formations. In some areas, there is an outcropping of till which are deposited on uplifted bedrock areas. These till deposits were formed by advancing glaciers and may have been reworked at later stages of Baltic Sea Basin. Till areas makeup over 70% of the

soil surface in Finland. In southern Finland, the uppermost soils are predominantly fine-grained deposits. According to Gardemeister (1975), the fine-grained soils in Finland were deposited during the final stage of the Ice Age (late-glacial sediments) when glaciation was retrieving, or afterwards (postglacial sediments) when ice cover had completely melted out. The different clays of fine-grained sediments belong to the glacio-marine deposits and marine sediments of the Baltic Sea basin. The soil structure exhibit variations due to the evolutionary stages of the Baltic Sea, see Figure (3.2).

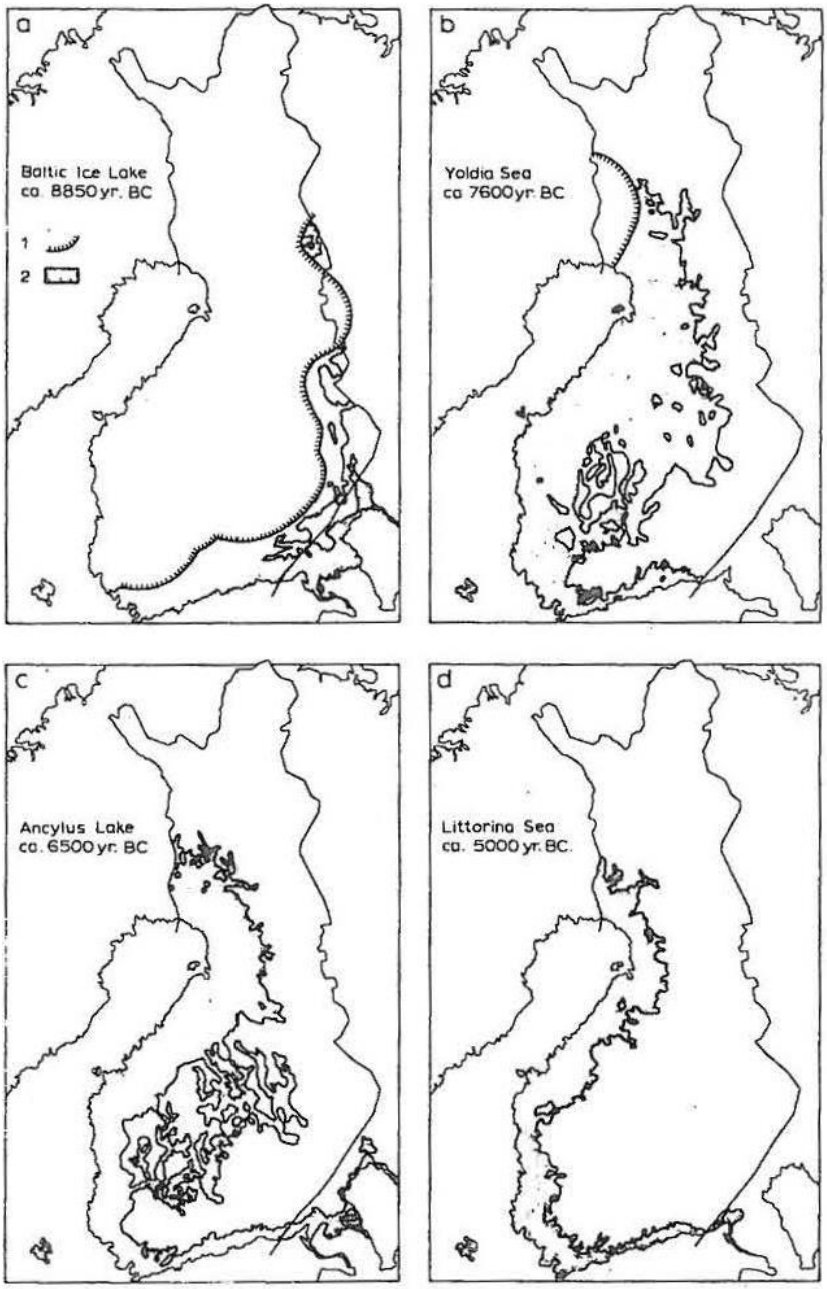

Figure 3.2: Main stages of the Baltic Sea basin (Gardemeister 1975).

The evolutionary stages includes;

a. The Baltic Ice Lake which constitutes the main part of the oldest sediments and this occurred during the late glacial period, between 10000 to 12000 years ago. The sediments are distinctly varved in structure with the bottom in many cases symmictic while the upper portion is diatactic. They contain glacial marine deposits.

b. Yoldia Sea in which the stratification of the deposited sediments is homogeneous in structure or is characterized by symmectic varving.

c. Ancylus Lake which is a freshwater lake formed as the land uplift occurred, breaking the link between the Yoldia Sea and the ocean. The sediments deposited in this stage are known to be homogeneous in structure.

d. Littorina Sea has the youngest deposited sediments and they are nearly homogeneous in structure. Sedimentation process which continues in the basin of the Baltic Sea began began 8000 years ago. These sediments primarily occur in coastal regions. Clays deposited in the saline Littorina sea contains more organic matter, sulphur and water-soluble salts than glacial clays.

These evolutionary stages comprise of different deposits or formation which are characterised by the types of depositional environments. According to Ojala et. al (2016), the Espoo area was an open embayment of the Baltic Sea Basin until the early times of the Litorina Sea. Hence fine-grained sediments are the predominant superficial deposits in the area. The Otaniemi area is predominantly present or Littorina deposits with an average elevation of 7m above sea level.

The Metsähovi area has a geological environment of an undulating granite bedrock surface covered by Quaternary till, silt, clay, and peat. The bedrock weathered top surface has been scraped off by Glaciation, uncovering well-polished outcrops of crystalline bedrock. According to field studies made by Hokkanen (2016), the lowermost soils comprise 0-2 m thick sandy tills with a mean thickness of 0.8 m overlain by glaciomarine silt and clay with an average elevation of 50m above sea level in this area. These deposits likely represent the Yoldia Sea and Ancylus Lake stages of the Baltic Sea basin which have been uplifted to their present altitude by the ongoing glacial rebound.

4 Soil sample characterization

It is necessary to understand the science of soil materials and some basics about soil properties when performing ERT survey. This chapter will provide a brief scope of fundamental properties of soil and soil classification.

4.1 Description of soil fundamental quantities

Soils are primarily made up of three different elements which are; solid, water, and air. In Figure (4.1), a visual and schematic diagram shows how soil occurs in its natural state. It is generally a mixture of four different components which is organic matter, mineral matter, water and air. Soils which is multiphase in its composition, occurs mainly in two phases as solid and liquid in which the solid phase acts as the skeleton of the soil, which is grains (or particles). The grains may consist of mineral matter or organic matter. Between the grains is the pore space also called voids that mainly include air and water occupying the pore spaces in soils. Air and/or water occupy approximately half the volume of soil. The density and unit weight, size of pore space, the water content in the voids as well as the composition varies for different soil types and affects the properties of the soil in different aspects.

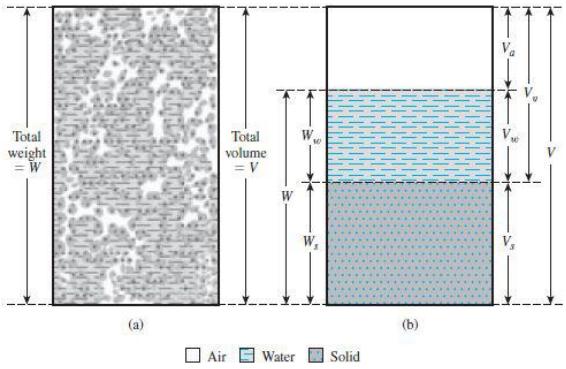

Figure 4.1: (a) Soil element in natural state; (b) three phases of the soil element(Das, 2009).

4.1.1 Density and Unit weight

Density which is mass per unit volume can be used to identify certain soil unique characteristic. The bulk density usually referred to as the density present in the naturally moist state (in-situ) is the combination of weight of the soil and weight of soil water in its natural structural arrangement in a given volume. Bulk density is determined by dividing the total weight of the soil by its volume, see Eq. (33). The variation in bulk density in different soil types is due to the difference in total pore space. Soils with fine textures have higher percentages of total pore space and hence smaller bulk density values. While compacted soils have lower percentages of total pore space and therefore higher bulk densities. This influences the soil ability to handle engineering structures. Although density and unit weight are used

interchangeably in some cases, the unit weight also known as the specific weight is the weight per unit volume of the soil. The weight W which is a force due to the acceleration due to gravity g on the mass M is given by the relation W = M.g.

There are different forms of unit weight and it is dependent on the level of water content in the sample. When the soil sample is completely dry, and weight is only that of the solid grains, it is referred to as dry unit weight, see Eq. (34). when the soil sample is completely saturated, that is the pore spaces are filled with water, it is referred to as saturated unit weight, see Eq. (35)(Craig, 2004). When the soil is below groundwater level there is an upthrust acting on the soil, and this is known as buoyant unit weight according to Archimedes principle, see Eq. (36). Equation see Eq. (37) shows the compact unit weight.

$$\rho = \frac{M}{V} \tag{33}$$

where:

ρ = bulk density

M = total mass (M = Ms + Mw)

V = total volume (V = Vs +Vv)

$$\gamma_d = \frac{W_s}{V} \tag{34}$$

where:

γ_d = dry unit weight

W_s = weight of solids

V = total volume

$$\gamma_{sat} = \frac{W_s + W_w}{V} \tag{35}$$

where:

γ_{sat} = saturated unit weight

W_s = weight of solids

W_w = weight of water

V = total volume

$$\gamma^{'} = \gamma_{sat} - \gamma_w \tag{36}$$

where:

$\gamma^{'}$ = buoyant unit weight

γ_{sat} = saturated unit weight

γ_w = Unit weight of water

$$\gamma_s = \frac{W_s}{V_s} \tag{37}$$

where:

γ_s = compact unit weight

W_s = weight of solids

V_s = volume of solids

4.1.2 Void Ratio, Porosity, and Relative density

The void ratio is one of the most fundamental properties of a soil, and it is the ratio of the volume of the voids to that of the volume of the solid, see Eq. (38). Porosity which is a similar fundamental property of soil is the ratio of the volume of the voids to the total volume of the soil, see Eq. (39) (Bell, 2007). The porosity is expressed as a percentage while the void ratio is expressed as a ratio (Craig, 2004).

$$e = \frac{V_v}{V_s} \tag{38}$$

where:

e = void ratio

V_v = volume of voids

V_s = volume of solids

$$n = \frac{V_v}{V} \tag{39}$$

where:

n = void ratio

V_v = volume of voids

V = total volume

The relative density or density index is used to characterize the density of a coarse-grained soil which expresses the relationship between the in-situ void ratio (e), or the void ratio of a sample, and the limiting values e_{max} and e_{min}, see Eq. (40). Hence from Figure (4.2), the relative density of soil in its densest possible state is 1 or 100% and the relative density in its loosest possible state is 0 (Craig, 2004).

$$D_r = \frac{e_{max} - e}{e_{max} - e_{min}} \tag{40}$$

where:

D_r = relative density

e_{max} = void ratio in the loosest state

e_{min} = void ratio in the densest state

e = void ratio

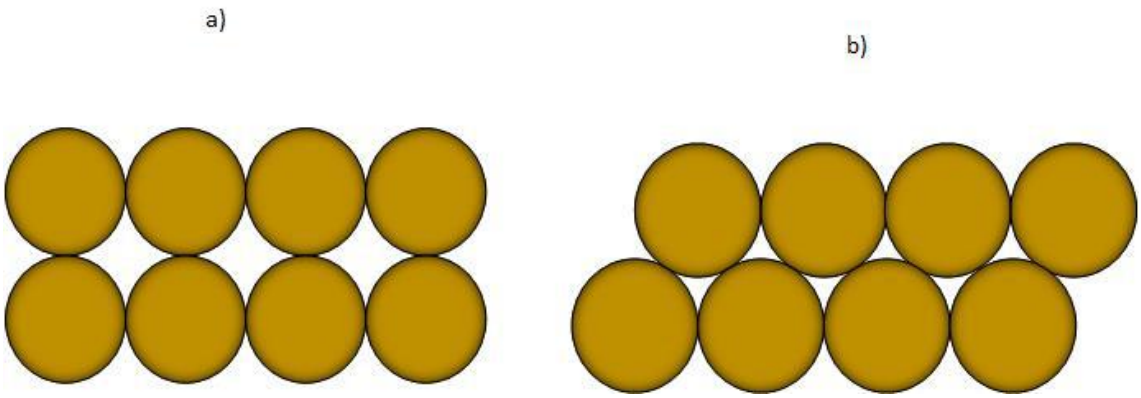

Figure 4.2: a) Loose and b) dense state of soil grain.

4.1.3 Water Content and Saturation

The water content also called the moisture content is one of the fundamental properties used to determine the engineering behaviour of soils. It is the ratio of the weight of pore water to the weight of the solids in a given mass of soil also known as gravimetric soil water content, see Eq. (41). This ratio is usually expressed as a percentage of the mass of the solid material in the soil sample (Bell, 2007). It is usually determined by weighing a given soil sample and then oven drying the sample for about 24 hours at a temperature of 105-110°C, after which it is reweighed. The amount of water or moisture in soil can also be measured as volumetric soil water content (VWC) which is the volume of water per volume of soil, see Eq. (42). The water saturation gives the relationship between the pore water volume and the volume of the pore space, see Eq. (43). The water saturation tells how much of the pore spaces are filled with

water. when the voids of soil are filled with water, it is referred to be a saturated soil (Craig, 2004).

$$w = \frac{M_w}{M_s} \tag{41}$$

where:

w = water content

M_w = mass of water

M_s = mass of solids

$$VWC = w * \rho \tag{42}$$

where:

VWC = volumetric water content

w = water content

ρ = bulk density

$$S_r = \frac{V_w}{V_v} \tag{43}$$

where:

S_r = water saturation

V_w = volume of water

V_v = volume of voids

4.1.4 Consistency

Soil consistency is the resistance of soils to deformation and rupture or the strength with which soil materials are held together. The Atterberg or consistency limits of fine-grained soils are founded on the concept that such soils can exist in any of four states depending on their moisture content (Craig, 2004). According to Das (2009), the moisture content at which the transition from solid to semisolid state takes place is defined as the shrinkage limit (w_S), the transition from semisolid to plastic state is the plastic limit (w_P), and from plastic to liquid state is the liquid limit (w_L). These parameters are also known as Atterberg limits, see Figure (4.3). The difference between the liquid limit and the plastic limit is known as the plasticity index, see Eq. (44). While the liquidity index can be determined by the given equation (45).

$$I_P = w_L - w_P \tag{44}$$

where:

I_P = plasticity index

w_L = liquid limit

w_P = plasticity limit

$$I_L = \frac{w - w_P}{w_L - w_P} \tag{45}$$

where:

I_L = liquidity index

w = water content

w_L = liquid limit

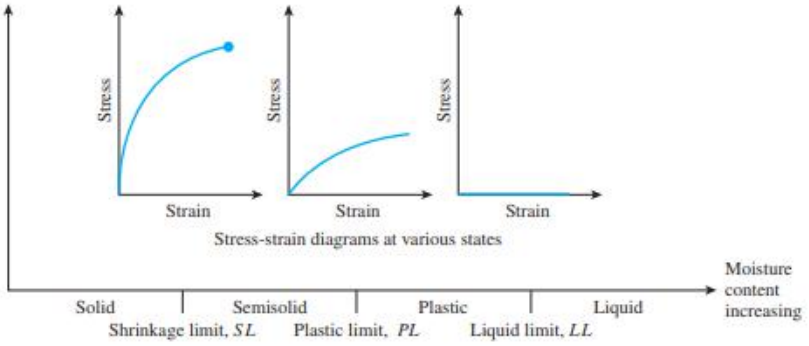

Figure 4.3: Atterberg limits (Das, 2009).

4.1.5 Grain Size and Grain Size Distribution

Grain size is also known as the particle size is one of the most important characteristics of soil as it is used to determine soil types. The grain size and size distribution of soil are much dependent primarily on the minerals that constitute the soil particles and, hence, the rock from which it is derived (Das, 2009). Soil ranges in different size fractions from clay, silt, sand, gravels, and organic soil particles are classified based on their size. Sand and gravel particles are large enough to be seen with the eyes and when rubbed between the thumb it gives a gritty feel. On the other hand, silt particles can barely be seen by the eye, and the smaller silt particles can be seen only with the aid of a microscope. Silt feels smooth when rubbed between the thumb and fingers. Clay includes the fraction smaller than silt and feels sticky and plastic when wet, and hard when dry.

There are two methods usually used to determine the particle size distribution in soil, that is, sieving and sedimentation. Sieving is done by putting the soil in a sieving machine according to size and amount and the result is plotted on a distribution graph where the horizontal axis indicates the particle size in a logarithmic scale and

the vertical axis indicates the proportion of particles smaller than the actual size in percentage. Grain size distribution in Table (4.1), shows the size of grains in percentages by weight according to the Unified Soil Classification System (USCS).

Table 4.1: Particle size distribution of soils (Bell, 2007).

Types of materials		**Sizes (mm)**
Boulders		Over 200
Cobbles		60 - 200
Gravel	Coarse	20 - 60
	Medium	6 - 20
	Fine	2 - 6
Sand	Coarse	0.6 - 2
	Medium	0.2 - 0.6
	Fine	0.06 - 0.2
Silt	Coarse	0.02 - 0.06
	Medium	0.006 - 0.02
	Fine	0.002 - 0.006
Clay		Less than 0.002

4.2 Soil Classification

The main purpose of soil classification is to arrange various types of soils into groups according to their engineering properties and various other characteristics. Soils with similar characteristics can be placed in the same group. However, the classification may be done to find the suitability of the soil for construction of engineering structures. Soils can be classified based on different properties like its texture and size, but the major characteristics used in classifying soils is the grain size. Several organizations have developed particle-size classifications which shows the particle-size classifications and Figure (4.4) shows a comparisson of these systems. Amongst these systems of classification, the Unified Soil Classification System is the most commonly used and universally accepted system. The Finnish geotechnical classification uses the SFS-EN ISO 14688-1, SFS-EN ISO 14688-2 standards and the GEO-clasification system. A brief discussion of the GEO-clasification system is discussed in this chapter.

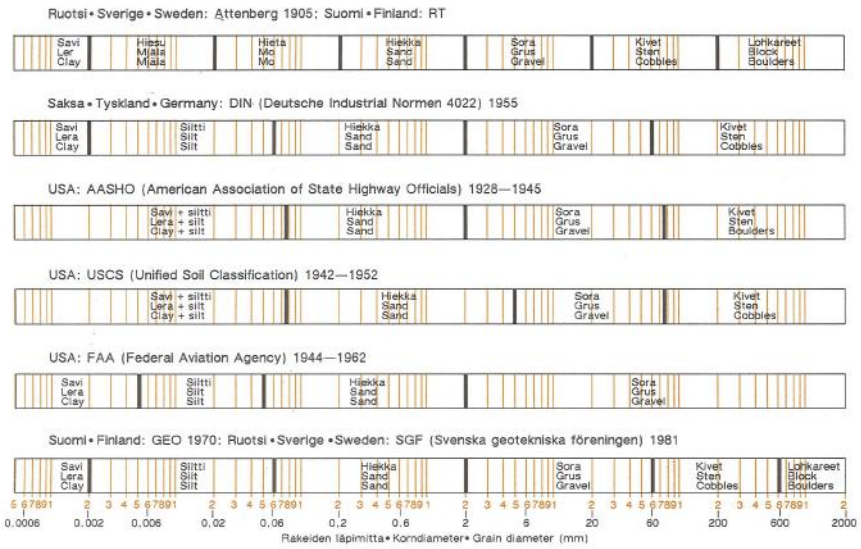

Figure 4.4: Comparison of the grain size classes of some soil classification (Alalammi, 1992).

4.2.1 GEO-classification

The geotechnical classification (GEO-classification) has been the main classification system used in Finland. In this classification, soil types are divided into mineral soils and organic soils. This division is dependent on the mode of their geological formation. Excluding clay, this classification uses the grain size distribution as a basis in the soil naming when 50% of the whole grain passes the sieve. When the soil contains a clay content of at least 30%, it is called clay.

The mineral soils are subdivided into three groups which provide the framework of the GEO-classification system, see Table (4.2). Figure (4.5) shows the GEO-classification curve with different soil types. Fine-grained soil types are described and named on the basis of clay content (<0.002 mm), see Table (4.3).

Table 4.2: Soil groups and soils according to GEO-classification (Alalammi, 1992).

Soil group	Abbrev.	Properties		Soil	Abbrev.	Fraction content, wt%			Grain size
		Humus, wt %	Fines $\leq$ 0.06mm, %			Clay	Fines	Gravel	d50 mm
Organic soils	E	>20		Peat Gyttja	Tv Lj				
Fine-grained soils	H	$\leq$ 20 Sorted	$\geq$ 50 Sorted	Clay Silt	Sa Si	$\leq$ 30 <30	$\geq$ 50	<5	$\leq$ 0.06
Coarse-grained soils	K		<50 Sorted	Sand Gravel	Hk Sr		<50 <5	$\leq$ 50 >50	>0.06 - 2 >2- 60
Tills	M	Non - sorted, composed of several grades		Silty till Sandy till Gravellly till	SiMr HkMr SrMr		$\geq$ 50 5 - 50 $\geq$ 5	$\geq$ 5 5 - 50 >50	$\leq$ 0.06 >0.06 - 2 >2

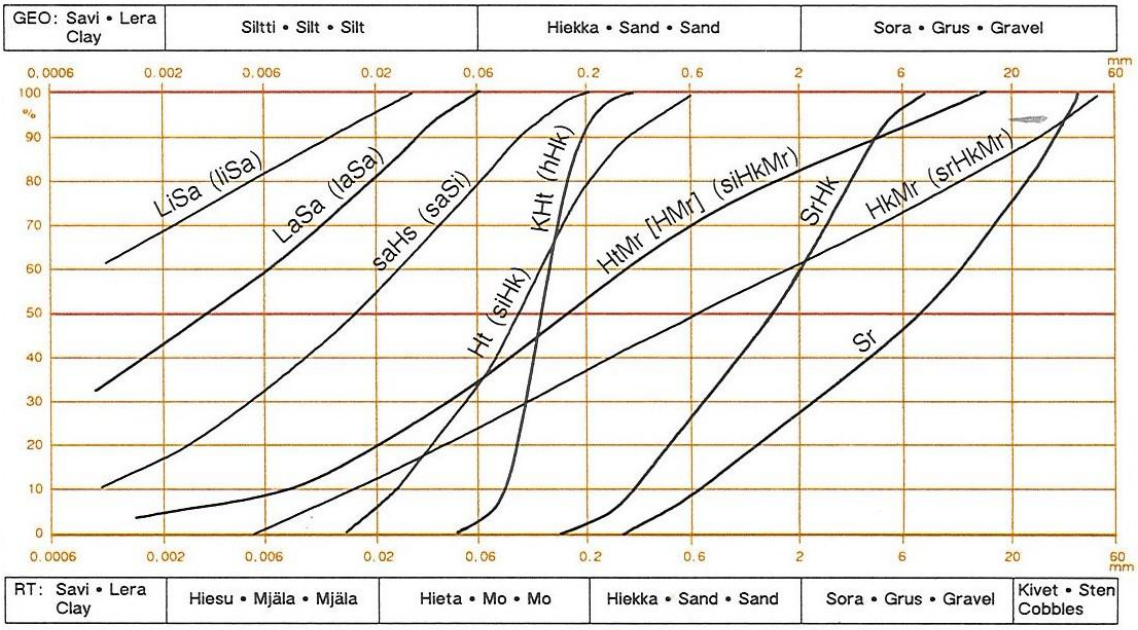

GEO-luokituksen mukainen lyhenne suluissa
Förkortning enligt GEO-klassifikationen inom parentes
Abbreviation by GEO classification in parentheses

LiSa = Lihava savi • Finlera • Fat clay
(liSa = Lihava savi • Finlera • Fat clay)

LaSa = Laiha savi • Grovlera • Lean clay
(laSa = Laiha savi • Grovlera • Lean clay)

saHs = Savinen hiesu • Lerig mjäla • Clay mjäla
(saSi = Savinen siltti • Lerig silt • Clay silt)

Ht = Hieta • Mo • Mo
(siHk = Silttinen hiekka • Siltig sand • Silty sand)

KHt = Karkea hieta • Grov mo • Coarse mo
(hHk = Hienohiekka • Fin sand • Fine sand)

HtMr = Hietamoreeni • Momorän • Mo till
[Maalajikartoituksessa • Vid jordartskarteringen • In soil mapping:
HMr = Hienoaineksinen moreeni • Morän med fint material • Till rich in fines]
(siHkMr = Silttinen hiekkamoreeni • Siltig sandmorän • Silty sandy till)

srHk = Sorainen hiekka • Grusig sand • Gravelly sand

HkMr = Hiekkamoreeni • Sandmorän • Sandy till
(srHkMr = Sorainen hiekkamoreeni • Grusig sandmorän • Gravelly sandy till)

Sr = Sora • Grus • Gravel

Figure 4.5: Grain size curves of mineral soils in RT and GEO classification (Alalammi, 1992).

Table 4.3: Description of fine-grained soils based on clay content (Korhonen et. al., 1974)

Clay content %	Name	Abbreviation
<10	does not affect the name	-
>10 .. 30	Clay silt	saSi
>30 .. 50	Lean clay	laSa
42	Fat clay	liSa

5 Data collection and analysis methods

In this study, both laboratory data and field data used in the analysis were obtained by ERT. Considering that the laboratory measurement was done to replicate soil conditions in its insitu state, the location of six soil samples was chosen to reflect different soil types. To get the desired soil type from the field, the topsoil was removed with a shovel. The topsoil which is the upper, outermost layer of soil, usually ranging from 13cm to 25cm and has the highest concentration of organic matter and microorganisms. Although the thickness of the topsoil ranges with location, it could exceed 25cm in thickness. After the topsoil is removed, the desired soil sample is dug and put in a container which is transported to the laboratory for treatment.

After the soil samples have been successfully collected, the samples are put in flat trays and dried in the oven at a temperature of 105°C for about 24 hours to ensure the soil moisture is almost 0%. This is done to remove all the soil moisture for the initial phase of the laboratory measurement. The oven-dried soil samples with blocks are then gently crushed and mixed to get an even moisture within the sample. To ascertain the soil types and their properties, different types of geotechnical soil test is performed on the samples.

5.1 Sieving and Hydrometer test

Soil samples collected for laboratory test were first classified using geotechnical laboratory procedures to identify the soil types. For this purpose, the soil samples were classified following the SFS-EN ISO 14688-1, SFS-EN ISO 14688-2 standards and Geo-classification. This classification standard mainly uses particle size distribution to identify soil types, see Table (5.1). According to this standard, the classification uses laboratory test results carried out following ISO 17892-1 to ISO 17892-12 standards. Amongst the Six soil samples, four are fine-grained samples and two are coarse-grained. In other to identify the fine-grained soil samples, a hydrometer test was performed. To identify the coarse-grained sample a sieving test was carried out in accordance with ISO 17892-4.

Table 5.1: Principles of soil classification (SFS – EN ISO 14688- 2:2018)

soil group	**Quantification**	**Denomination into soil groups**			**Further sudivision as appropriate by**
		Primary fraction (symbol)	**Composite fractions**		
very coarse	>50 % of particles by mass ≥200 mm	Boulders (Bo)	BOULDERS BOULDERS with cobbles	BOULDERS with finer soils	Requires special consideration
	>50 % of particles by mass <200 mm and ≥63 mm	Cobbles (Co)	COBBLES COBBLES with boulders	COBBLES with finer soils	
coarse	>50 % of particles by mass <63 mm and ≥2 mm	Gravel (Gr)	GRAVEL with cobbles GRAVEL sandy GRAVEL with cobbles	Sandy GRAVEL GRAVEL with clay and silt	Particle size distribution, Shape of grading curve, Relative density/ density index, Permeability
	>50 % of particles by mass <2 mm and ≥0,063 mm	Sand (Sa)	Gravelly SAND SAND	SAND with clay or silt	Mineralogy, Particle shape
fine	low plasticity or non-plastic	Silt (Si)	sandy SILT	sandy gravelly SILT sandy clayey SILT	Plasticity, Water content, Strength, Sensitivity, Compressibility, Stiffness, Clay mineralogy
			clayey SILT, silty CLAY		
	plastic	Clay (Cl)	Sandy gravelly CLAY Organic SILT Organic CLAY		
organic		PEAT (Pt) GYTTJA (Gy) DY (Dy) HUMUS (Hu)	Sandy PEAT sandy clayey GYTTJA		Requires special consideration
Anthropogenic soil		Made Ground	Placed without control	Synthetic material or Reworked natural materials (such as crushed, graded or washed materials	Requires special consideration As for natural soils
		Fill	Placed with control	Synthetic material	

5.1.1 Sieving test description

Sieving test is a simple means to measure particle size of dry relatively flowing materials. For this purpose the items required to carry out this test are;

- Test sieves conforming to ISO 3310-1 and ISO 3310-2
- Mechanical sieve shaker
- Scoop
- Sieve brushes

- Corrosion resistant trays
- Scale
- Drying oven
- Timer.

The samples are placed in the oven at 110 °C for 24 hours to remove the soil water after which it is allowed to cool. A measure tray is placed on the scale to get the tare weight of the tray then the test sample is placed on the tray and weighed. It is recommended to use a wide range of sieve sizes to eliminate discontinuities in the grading curve. The sieves are first cleaned with the sieve brushes to remove residual particles from the previous test, then it is arranged in order of decreasing size opening from top to bottom to form a sieve stack which is placed on a sieve pan, see Figure (5.1). The test sample is poured from the top of the sieve stack and covered with a stack cover. The weight of the sample is usually chosen according to Table (5.2).

Table 5.2: Recommended minimum masses for sieving.

Particle diameter D_{max}[a] mm	**Recommended minimum masses**[b] g
<2,0	100
2,0	100
6,3	300
10	500
20	2 000
37,5	14 000
63	40 000

[a] Maximum diameter of soil particles, excluding any discrete coarser particles present.

[b] Using a test specimen smaller than the recommended minimum mass indicated requires discretion, although it may be adequate for the purpose of the test.

The sieve stack is placed in the mechanical sieve shaker for a sufficient time commonly, 10, 15 or 20-minute are used as arbitrary sieving intervals so that not more than 1% by mass of the material retained on any individual sieve will pass that sieve during 1 minute of sieving. When sieving is complete, the mass weight of the sample retained on each sieve size is measured and recorded to the nearest 0.1g. The total mass of the sieved sample should match closely to the original mass of the test sample before sieving was done. If the amounts differ by 0.3%, based on the original dry sample mass the test should be repeated. The results of the sieving process are

usually plotted as a grading curve which gives the percentage by mass of each size fraction.

Figure 5.1: Sieve stack assembled on a sieve shaker (*Photo: Omoghomion Oredia 22.07.2019*).

5.1.2 Hydrometer test description

The Hydrometer test also known as Aerometer test in which soil particles are separated into size classes by the gravitational settling in a liquid, where the different size classes settle at different rates based on stokes law. This test is carried out on samples with particle size less than 0.063mm. Particles less than 0.063mm can not be sieved because they carry charges on their surface and have the tendency to stick to the sieve surface or the particles stick to each other. The items required to carry out this test are;

- Sedimentation Cylinder (Jar)
- Sodium Hexametaphosphate
- Hydrometer
- Dispersion Cup
- Soil Dispersion Mixer
- Thermometer
- Timer.

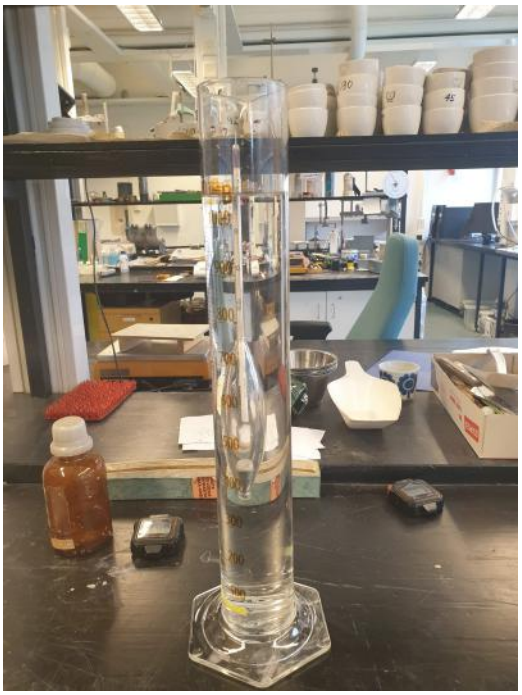

Figure 5.2: Calibration of hydrometer for zero correction factor (*Photo: Omoghomion Oredia 22.07.2019*).

Figure 5.3: Hydrometer test sedimentation Cylinder (*Photo: Omoghomion Oredia 22.07.2019*).

The test is started by weighing 50g of 0.063mm sieved dried fine-grained soil sample which is mixed with 150ml of dispersing agent (Sodium Hexametaphosphate) in a jar and allowed to sit for 24 hours. The dispersing agent separates the particle flocs which is required for the sedimentation process. After mixing with the dispersing agent, the sample is stirred with the mechanical stirrer for a few minutes then it is transferred to a sedimentation cylinder. Distilled water is added to the mixed sample to make the suspension volume 1000ml after which it is agitated to mix the soil suspension homogenously. The suspension passing the 0.063mm sieve is transferred to a sedimentation cylinder. After the first minute, a calibrated hydrometer showed in Figure (5.2) is inserted in the Sedimentation Cylinder and the first reading is taken from the hydrometer staff at the top of the meniscus of the suspension. The thermometer is inserted in the suspension to take the temperature reading as well. The readings are taken at time intervals of 4 min, 8 min, 30 min and 1 h, 2 h, 6 h and 24 h. Figure (5.3) shows the sedimentation process of the 4 fine-grained samples used for this study.

5.2 Resistivity experiment in Laboratory

The ERT laboratory test for this study was done using the Wenner array system with 5cm spacing for both current and potential electrodes. For this test to be carried out the items required are;

- ABEM Terrameter SAS 300C

- 12V battery
- 2 Wooden boxes 40.2cm x 26.7cm x 24cm, 40.6cm x 27.2cm x 22.4cm
- 4 Silver Chloride (AgCl) electrodes
- Plastic bags
- Treated soil samples
- Tap water (Resistivity: 52Ωm)
- Temperature controlled room.

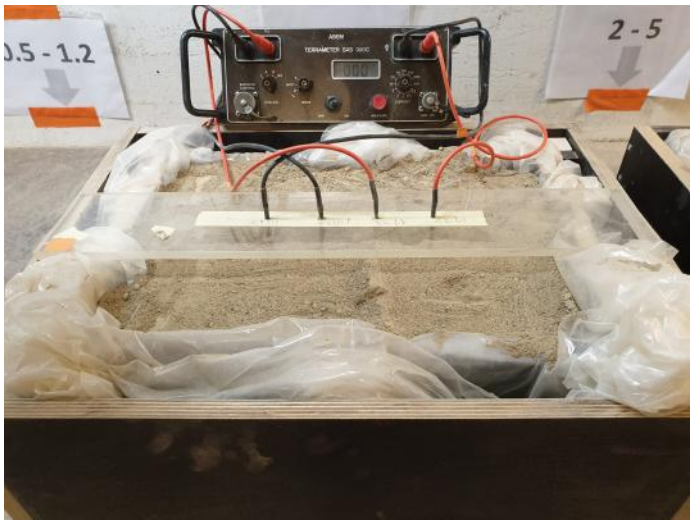

Figure 5.4: ERT laboratory test setup. Side-view (*Photo: Omoghomion Oredia 24.10.2019*).

Figure 5.5: ERT laboratory test setup. Top-view (*Photo: Omoghomion Oredia 24.10.2019*).

The Laboratory experiment was done to determine the resistivity of soil at different temperatures and different water content to define the effect of their change to ERT. The soil samples are kept in the temperature-controlled room 48 hours before the first measurement to ensure the soil temperature is even. At the initial phase, the laboratory items are set up with the interior of the wooden boxes lined up with the plastic bags to make it watertight and prevent the soil samples to lose its water content. The soil sample is poured into the box and compacted for about 5 minutes to reduce the air voids and increase grain contact while the soil sample surface is made homogeneous. The terrameter is connected to the 12V battery power source and the 4 AgCl electrodes are pushed into the soil sample. To ensure the electrodes are vertical and evenly spaced, a transparent plastic slab with the electrode spacing holes drilled is used to support the electrodes. The terrameter is switched on and the measure knob is pushed to start the measurement which gives the resistance value of the soil sample on the LED display, see Figure (5.4) and Figure (5.5). The ABEM terrameter SAS 300C used for the measurement has a range of measurement cycles of 1, 4, 16, 64 but for this test 4 cycles were taken for each measurement and the average taken as the resistance value.

This measurement is done on the six soil samples at different temperature values and different soil water content. Each round of measurement contains a resistance value at a specific water content range and different temperature values. Tap water is added to the soil samples to increase the water content and the test is repeated at different soil temperature values for each round. The resistivity and pH of the tap water were measured at room temperature of 20°C. The water content for each measurement round was estimated by weighting after which it is converted to VWC using Eq. (42). After each measurement, a portion of the soil is taken from the box in a cup which is weighed and put in the drying oven for 24 hours after which it was weighed again, see Figure (5.6) and Figure (5.7).

Figure 5.6: Wet Soil samples in Oven (*Photo: Omoghomion Oredia 24.10.2019*).

Figure 5.7: Soil samples after oven drying (*Photo: Omoghomion Oredia 24.10.2019*).

The resistivity laboratory experiment was done to characterize the resistivity of the soil samples at different temperatures and with different VWC to define the effect of their change to ERT. The resistivity of the tap water used to regulate the VWC of the soil samples is measured to be 52Ωm. Also the TDS in the tap water is estimated to be 125 mg/l using Eq. (16)

5.3 Field measurements

In this field survey, the Dipole-dipole array system was used for the ERT mapping. This array was chosen due to its ease of deployment and depth penetration. The field test was done in the same location where the O.T3 sample was taken. The array line was set up in a way that the point where the O.T3 soil sample was extracted lies 43m from the first electrode in the array. This is done to correlate the laboratory data with the data from the field test. For this field study to be carried out the items required are listed below, see Figure (5.8).

- ABEM terrameter SAS 4000
- 12V battery
- Hammers
- Connection cables with takeouts, on reel
- Steel electrodes
- Decagon Em50 Datalogger

Figure 5.8: ABEM LUND Imaging System and Accessories used for ERT mapping (*Photo: Omoghomion Oredia 29.10.2019*).

In this field measurement, 18 electrodes were used with a 5m spacing giving a 90m sampling area. The electrodes are installed by pushing them vertically into the soil with the aid of the hammer. The connection cables are unreeled and the corresponding takeout is connected to the electrode with the aid of a rubber clip, see Figure (5.9). This method of connection gives better contact between the electrodes and takeouts when compared to the conventional alligator head connection clip. The connection cable is connected to the ABEM terrameter SAS 4000, which serves as the base station after which the Terrameter is connected to the car battery and switched on. The Dipole-dipole array protocol is selected from the terrameter and an electrode connection check is done before the measurement is started. See Terrameter SAS1000/4000 LUND Imaging System Introduction Manual for a detailed explanation.

In order to get a trend in the resistivity value of the soil, this measurement was done once every month for 5 months from June to October. In order to monitor the seasonal changes in the temperature and moisture of the soil, a Decagon 5TE Data logger was introduced, see Figure (5.10). The logger sensor was buried at the depth of 60cm which corresponds to the same depth at which O.T3 soil sample was collected. The data logger was set to measure temperature and VWC at a 10 minutes interval.

Figure 5.9: Steel electrode connected to a takeout with a rubber clip (*Photo: Omoghomion Oredia 29.10.2019*).

Figure 5.10: Em50 Datalogger measuring soil temperature and moisture (*Photo: Omoghomion Oredia 29.10.2019*).

To measure the insitu soil matrix resistivity, a replication of the laboratory ERT measurement is carried out in the field. A 40.2cm x 26.7cm hole is dug to a depth of 60cm at the same location where the O.T3 sample was collected, see Figure (5.11). ERT measurement is taken using 4 Silver Chloride (AgCl) electrodes with 5cm spacing as explained in Section 5.2. The hole is left for several hours to let the pore water gather after which a sample of the pore water is collected in a capped bottle and placed in a cold room for about 8 hours then taken to the laboratory to measure its resistivity and pH, see Figure (5.12). The pH and resistivity of the pore water are measured directly at room temperature on the 1st of November 2019 using a pH meter without filtering the pore water sample.

Figure 5.11: Replication of laboratory ERT measurement in the field (*photo: Omoghomion Oredia 01.11.2019*).

Figure 5.12: Field pore water extraction (*photo: Omoghomion Oredia 01.11.2019*).

6 Results

This chapter includes the results from the sieving test, hydrometer test, ERT field and laboratory tests described in chapter 5. Graphs and charts depicting the correlation of test values are provided for each method used.

6.1 Sievings and Hydrometer tests result

The values got from the sievings and hydrometer test for all the soil samples provided in Appendix A are plotted to get a particle size distribution curve shown in Figure (6.1). To obtain the fraction passing the sieves, Eq. (46) is used.

$$f_n = 100\% - [\frac{m_{ss1} + m_{ss2} + .. + m_{ssn} + m_{s1} + m_{s2} + .. + m_{sn}}{m} * 100\%] \tag{46}$$

where:

f_n = fraction passing the given sieve size, n (%);

m_{ss1}, m_{ss2} = masses of soil retained on each sieve for sieves sizes greater than the separation sieve (if used) after scaling for each riffle stage (g);

m_{ssn} = mass of soil retained on sieve size, n, for sieve sizes greater than or equal to the separation sieve size (if used) after scaling for each riffle stage (g);

m_{s1},m_{s1} = masses of soil retained on each sieve larger than sieve size, n, for sieve sizes smaller than the separation sieve after scaling for each riffle stage (g);

m_{sn} = mass of soil retained on sieve size, n, for sieve sizes smaller than the separation sieve size after scaling for each riffle stage (g);

m = total dry mass of the initial soil specimen (g).

To determine the name of the different soil samples, the values from the seive and hydrometer test is plotted on a gradation chart according to GEO-classification, see Figure (6.1). The naming is also done using gradation chart according to SFS-EN ISO 14688-2:2004, see Figure (6.2). This chart classifies the soil samples based on gradation only and it gives the values of the percentage of fines, clay, sand, and gravel. For detailed explanation on how the values for the hydrometer test was calculated in Appendix A, see SFS-EN ISO 17892-4:2016.

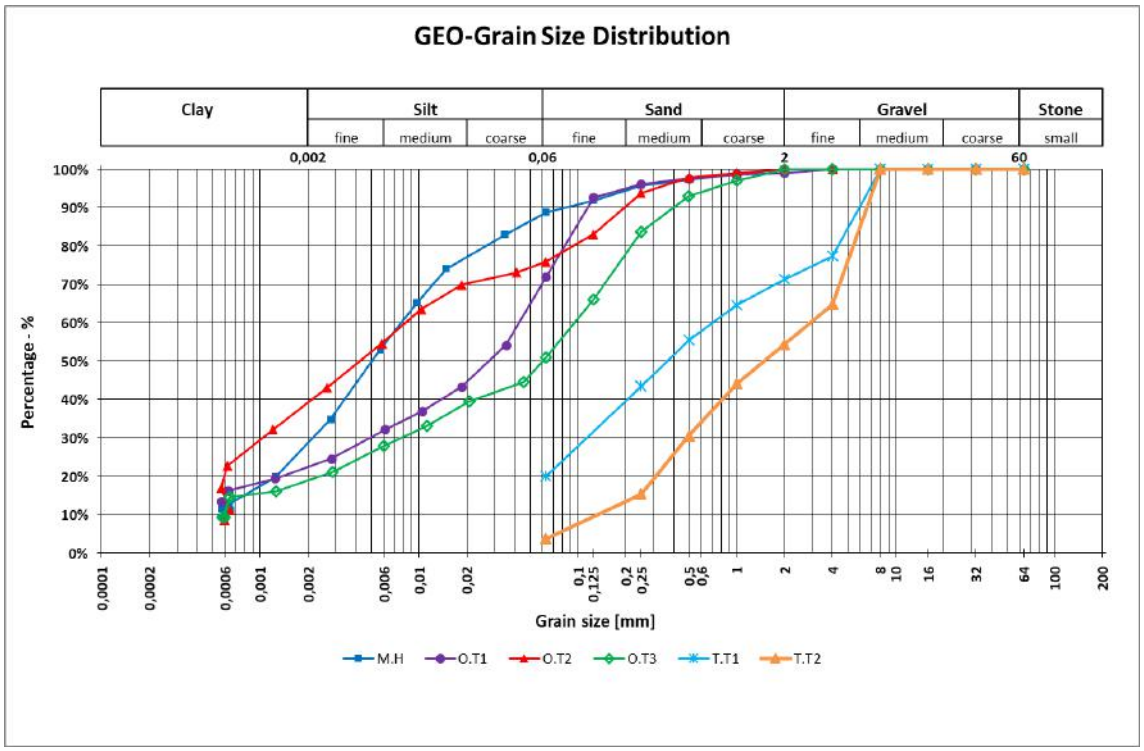

Figure 6.1: Soil samples particle size distribution curves according to GEO-classification.

The names and a summary of the percentage of fines, clay, sand, and gravel of the six soil samples are given in Table (6.1). There are four cohesive soil samples; M.H, O.T1, O.T2, O.T3, and two friction soil samples; T.T1, T.T2.

Table 6.1: Soil samples gradation and names

Soil sample	**Gravel content in (%) (2mm - 63mm)**	**Sand content in (%) (0.063mm - 2mm)**	**Fines content in (%) (<0.063mm)**	**Clay content in % of mass of coarse and fine soil (grain size <63 mm)**	**SFS-EN ISO 14688**	**GEO classification**
M.H	0.00	11.26	88.74	27.19	silty Clay (siCl)	Clay silt (saSi)
O.T1	0.98	27.12	71.90	21.90	sandy silty Clay (sasiCl)	Clay silt (saSi)
O.T2	0.00	24.10	75.90	38.59	sandy Clay (saCl)	Lean clay (laSa)
O.T3	0.00	49.06	50.94	18.41	sandy silty Clay (sasiCl)	Clay silt (saSi)
T.T1	28.71	51.31	19.98	0.00	gravel clayey Sand (grclSa)	Sandy till (HkMr)
T.T2	45.58	50.67	3.75	0.00	gravel Sand (grSa)	Gravelly sand (srHk)

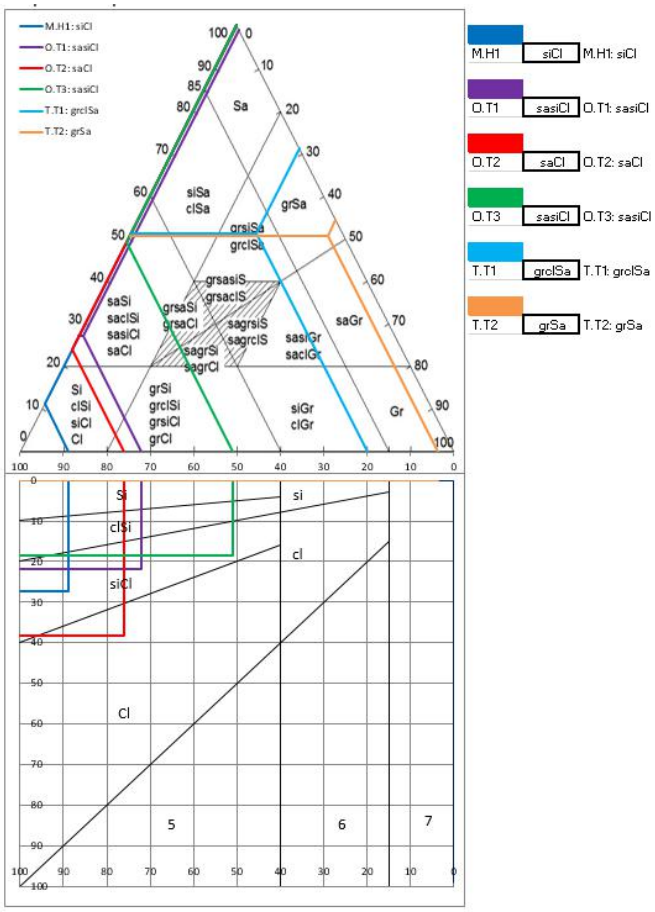

Figure 6.2: Classification of soils, based on gradation according to ISO 14688-2:2018.

6.2 Laboratory experiment

The soil resistance data from the laboratory experiment is first converted to apparent resistivity. This is done by calculating the geometrical factor K using Eq. (20) after which it is multiplied by the resistance value using Eq. (21) for each round. The VWC were maintained and measured as described in section 5.2 using Eq. (41). The results for the calculated apparent resistivity including the data from all the rounds of measurement for each sample is provided in Appendix B. This apparent resistivity value is equivalent to the true resistivity value because the laboratory measurements are done in a homogeneous soil surface as explained in section 2.1.1.

The values of the apparent resistivity are plotted against the values of the soil temperature at the different VWC level in each round for the six soil samples. The results show that all samples are dependent on VWC and the smaller VWC the more dependent resistivity is on temperature (gradient of trend lines), see Figure (6.3) to Figure (6.8). With low VWC, a high gradient is developed when compared with high VWC the relations become almost flat. The ratio between the gradients of the trend lines at high VWC and low VWC are 1:58, 1:20, 1:9, 1:47, 1:8, 1:20 for M.H, O.T1, O.T2, O.T3, T.T1, T.T2 respectively. These relations show the extent of how

each sample apparent resistivity is dependent on temperature change when the VWC increases with M.H having the highest dependency. Since both M.H and O.T3 are similar soil type (clay silt) from the two different locations in the study area, there is a substantial 21% difference in their dependency on temperature change. This suggests that there is a substantial difference in the resistivity of the soil matrix and soil TDS as both have the same pore water (tap water).

At the highest VWC level the different soil samples have reached saturation. At this saturation level, the effect of changing the VWC is minimal. To estimate the effect of soil temperature change on the apparent resistivity value for each soil sample when it is saturated, the % decrease in apparent resistivity per 1°C increase in soil temperature between 2°C and 14°C is calculated for each sample, see Table (6.2).

Also from Figure (6.3) to Figure (6.8), the % decrease in apparent resistivity per 1% increase from the highest to the lowest VWC at 8°C is calculated for each sample, see Table (6.2). This temperature value falls within the mean annual temperature in Southern-Finland which is about 5.5°C to 8°. It also corresponds to the mean temperature in the subsurface/groundwater zone. This is to show how the soil resistivity values are influenced by VWC.

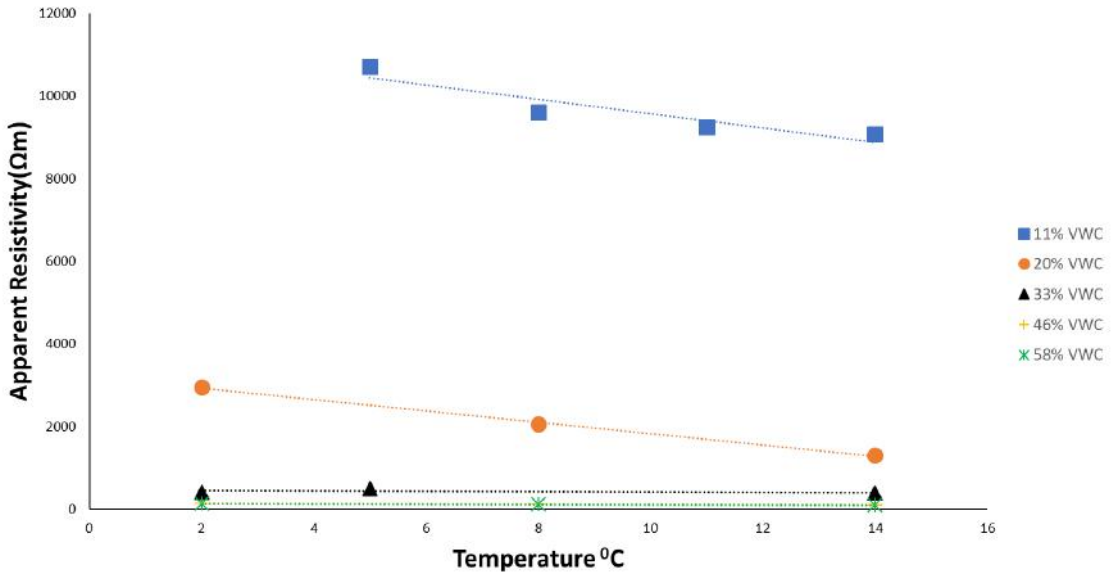

Figure 6.3: Relationship between laboratory measured Apparent resistivity and Soil temperature at different water content level for M.H.

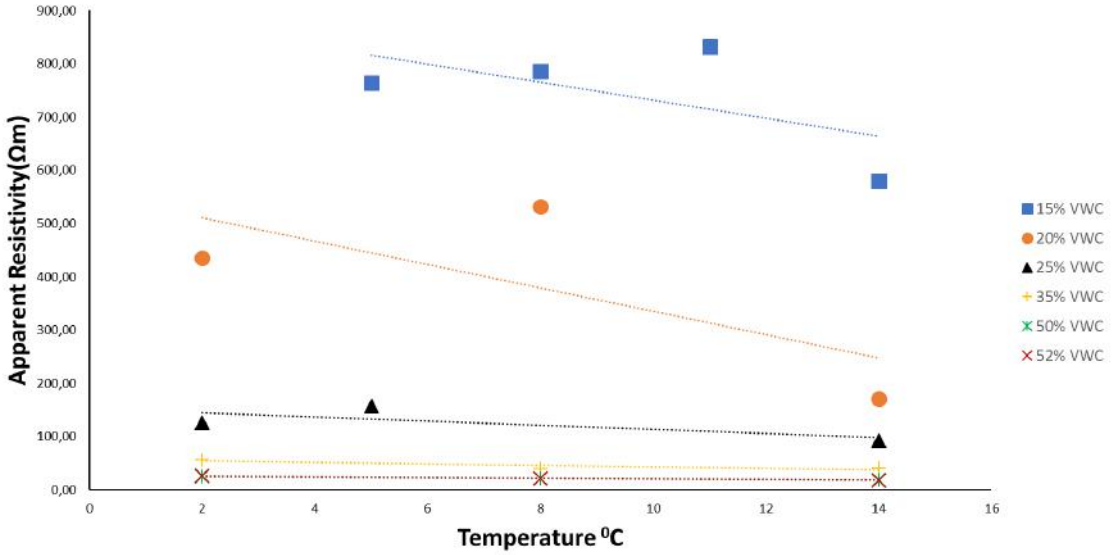

Figure 6.4: Relationship between laboratory measured Apparent resistivity and Soil temperature at different water content level for O.T1.

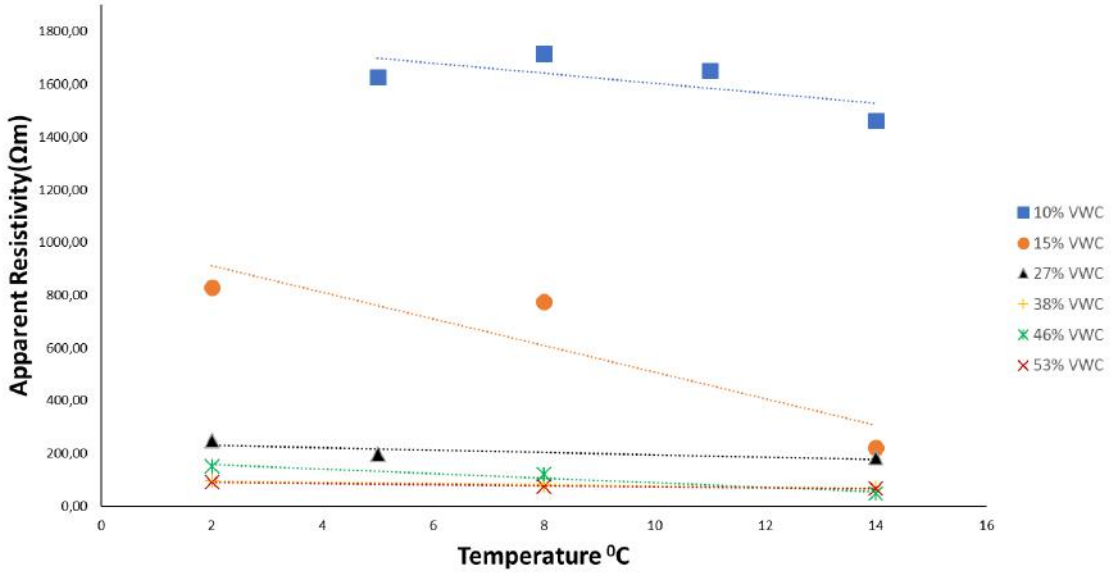

Figure 6.5: Relationship between laboratory measured Apparent resistivity and Soil temperature at different water content level for O.T2.

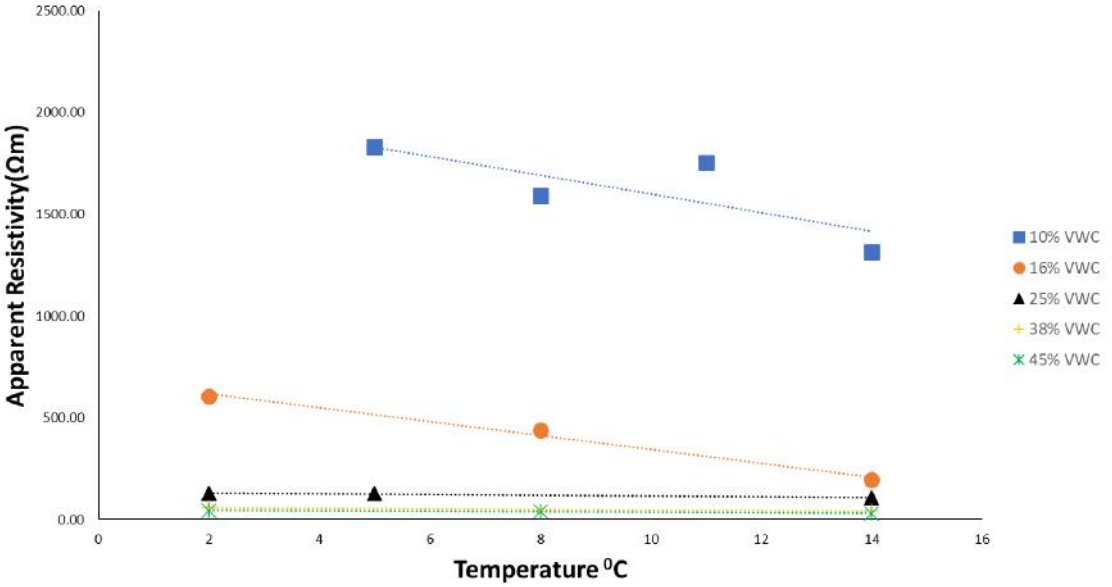

Figure 6.6: Relationship between laboratory measured Apparent resistivity and Soil temperature at different water content level for O.T3.

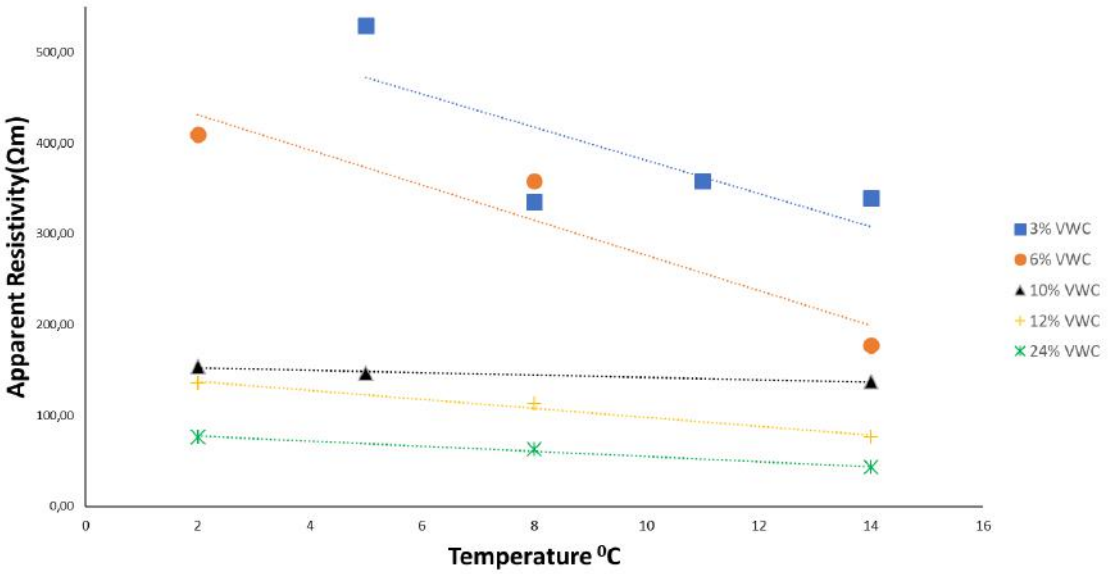

Figure 6.7: Relationship between laboratory measured Apparent resistivity and Soil temperature at different water content level for T.T1.

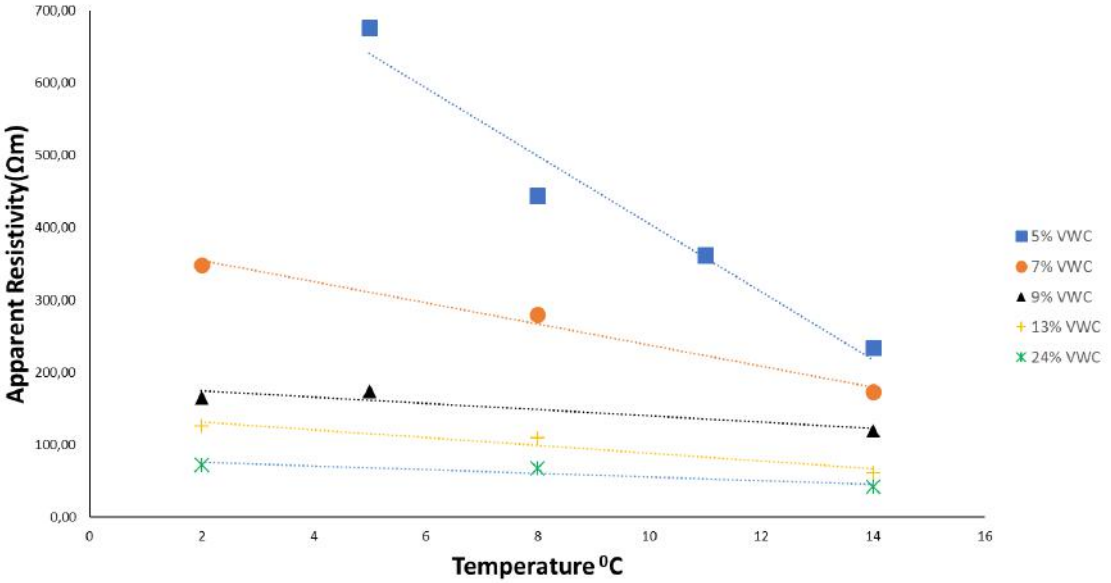

Figure 6.8: Relationship between laboratory measured Apparent resistivity and Soil temperature at different water content level for T.T2.

Also, the water content values are plotted against apparent resistivity for each sample, see Figure (6.9) to Figure (6.14). In the plots, the values of apparent resistivity without the tap water resistivity is plotted alongside the apparent resistivity values with tap water resistivity. The tap water resistivity value can be subtracted from the measured laboratory soil resistivity using Eq. (47). This equation can be applied when the soil is fully saturated and it gives an approximation of the minimum resistivity for the sample after the effect of tap water has been removed.

$$\rho_{wT} = \rho_{LS} - \rho_T \tag{47}$$

where:

ρ_{wT} = laboratory soil resistivity without tap water resistivity

ρ_{LS} = laboratory soil resistivity with tap water resistivity

ρ_T = tap water resistivity

The ration ρ_T/ρ_{LS} is actually (ρ_{LS}-ρ_{wT})/ρ_{LS} and therefore an estimate how much ρ_{wT} can change due to infiltration of fresh water (precipitation) into unsaturated soil. This relation shows the sensitivity of the different soil samples to pore water in ERT measurement, see Table (6.2). The pH value of the tap water used for this test range from 6.9 - 7.15 which corresponds to a neutral PH value. This means the tap water is not contaminated with extra ions which enhance the conductivity of pore water.

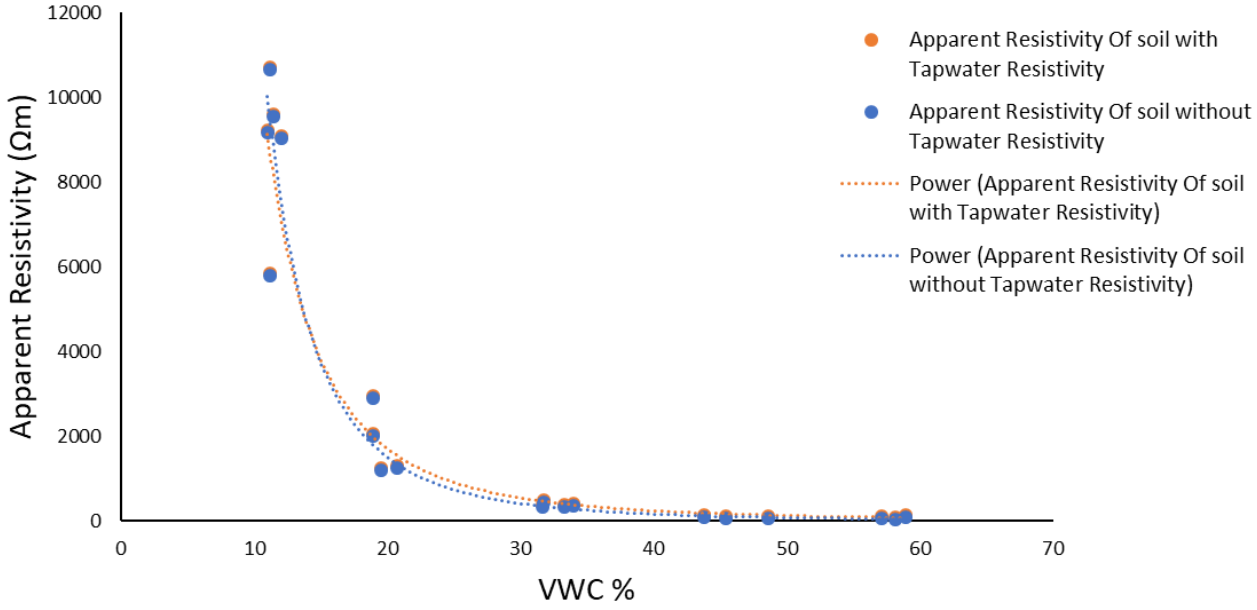

Figure 6.9: Correlation between water content and laboratory apparent resistivity for M.H.

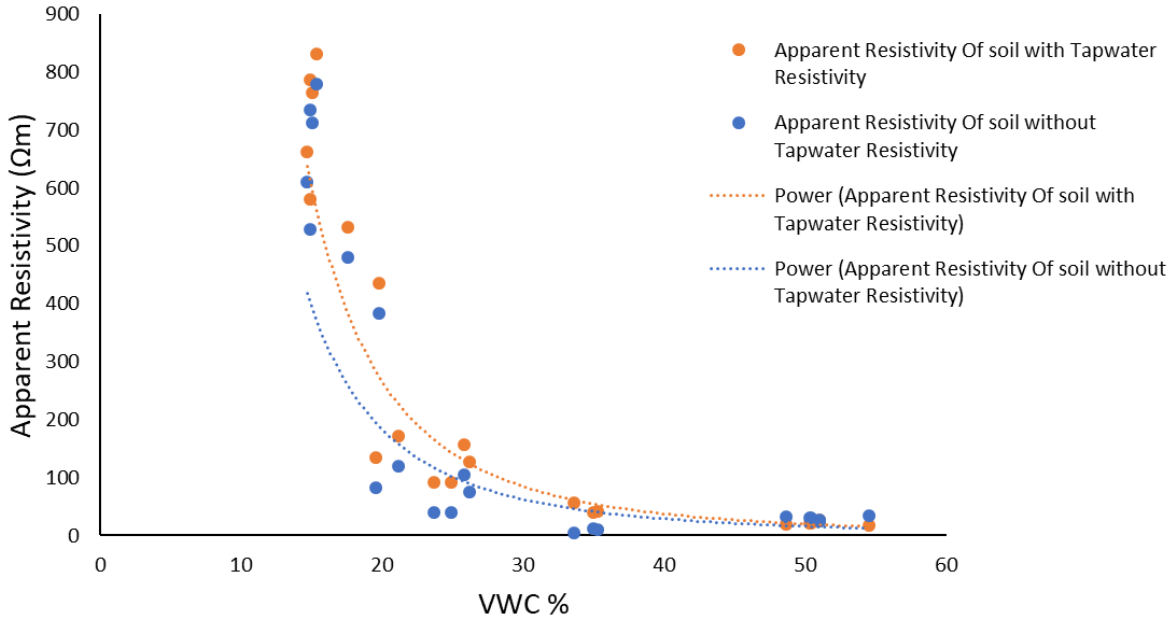

Figure 6.10: Correlation between water content and laboratory apparent resistivity for O.T1.

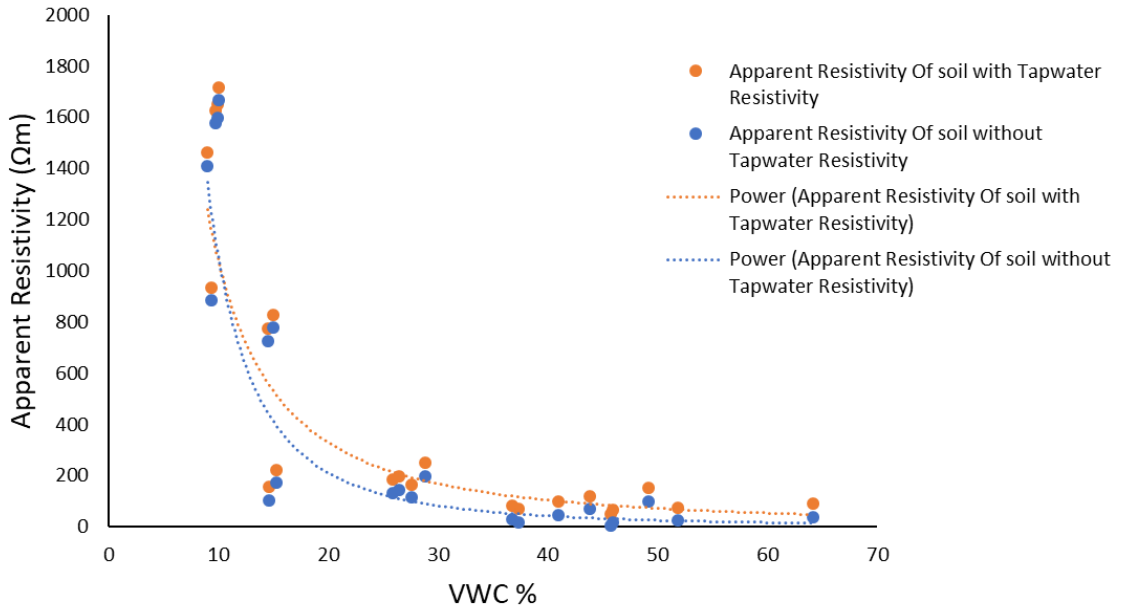

Figure 6.11: Correlation between water content and laboratory apparent resistivity for O.T2.

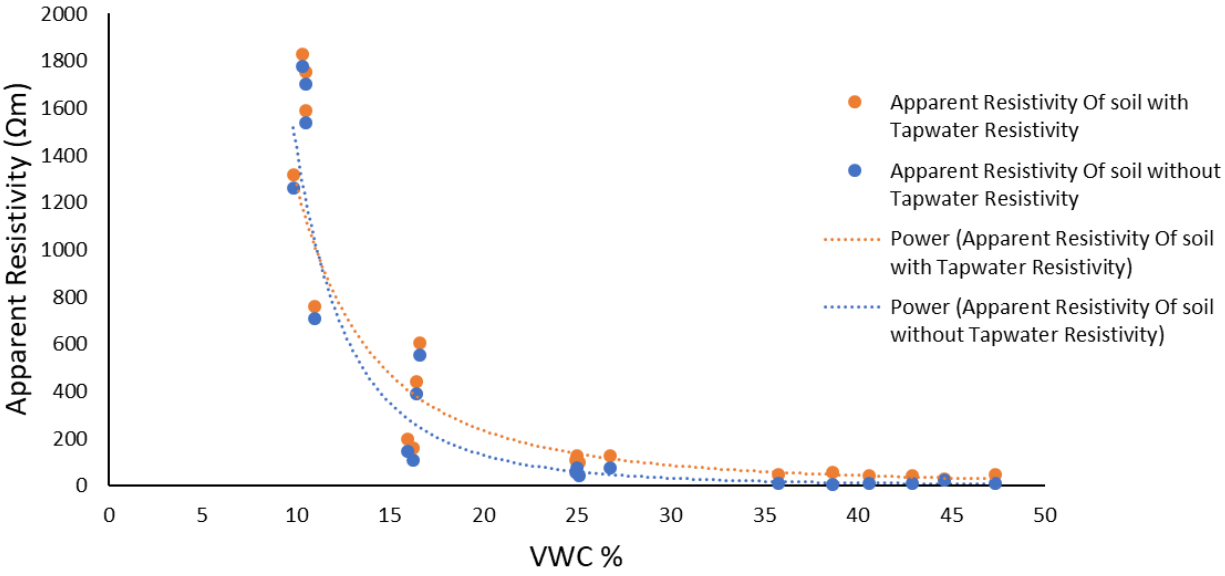

Figure 6.12: Correlation between water content and laboratory apparent resistivity for O.T3.

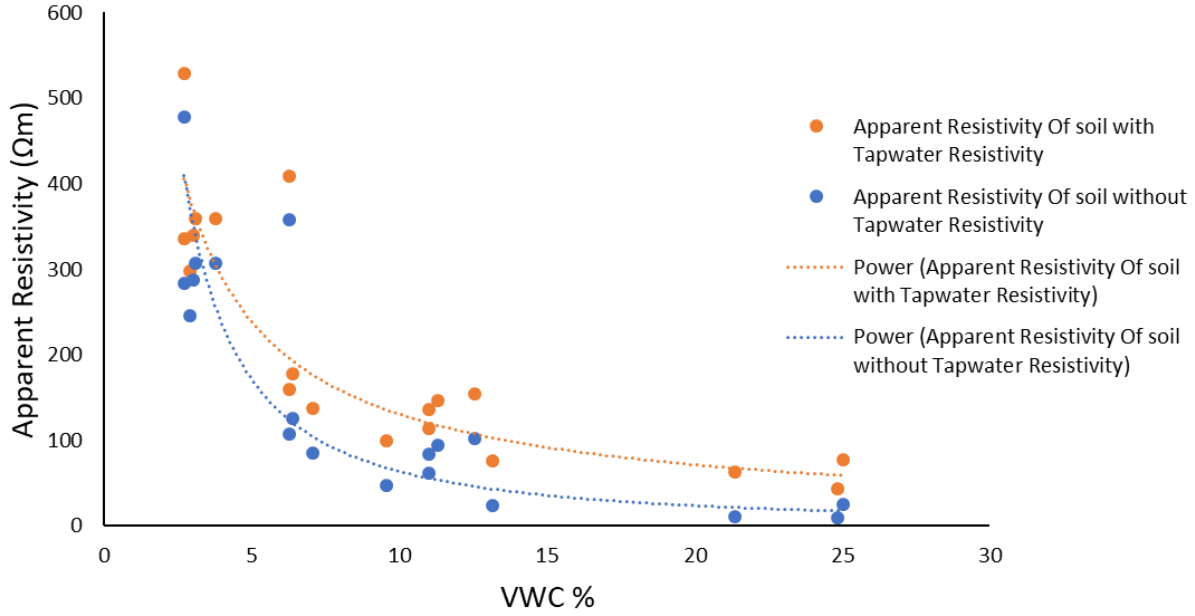

Figure 6.13: Correlation between water content and laboratory apparent resistivity for T.T1.

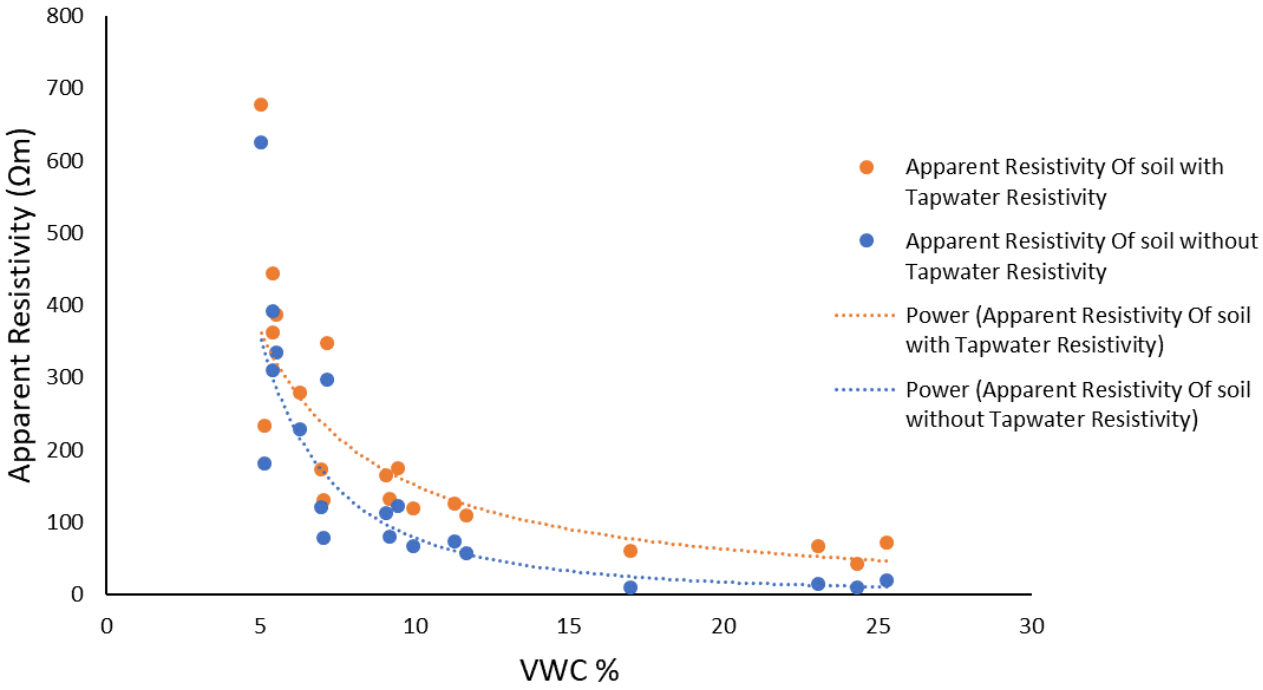

Figure 6.14: Correlation between water content and laboratory apparent resistivity for T.T2.

Table 6.2: Effect of temperature and water content on laboratory ERT

Soil Sample	Soil Type (GEO-Classification)	% decrease in saturated soil resistivity per 1°C increase in temperature	Resistivity % decrease per 1% VWC increase from unsaturated to saturated soil	% difference btw ρ_{LS} and ρ_{wT}
M.H	Clay silt (saSi)	2%	3%	0.62%
O.T1	Clay silt (saSi)	2.6%	4.5%	6.33%
O.T2	Lean clay (laSa)	2.17%	4%	4.12%
O.T3	Clay silt (saSi)	2.75%	4.5%	3.42%
T.T1	Sandy till (HkMr)	4%	8.7%	25.18%
T.T2	Gravelly sand (srHk)	4%	8.7%	12.91%

6.3 Field studies result

The data obtained from the field measurement described in Section 5.3 was transferred from the ABEM tetrameter to a computer using SAS4000 utility software. The data was processed and analyzed using RES2DINV software to provide an inverse model that gives an approximate analysis of subsurface resistivity values. This software provides an inverse model of the data based on the smoothness constrained least-squares method. RES2DINV is popularly adopted by researches as an electrical resistivity data processing tool and it is known worldwide for its user-friendliness, See Loke (2001) for a detailed description of the different variations of the smoothness constrained least-squares method utilized by the RES2DINV software. The inversion model produced by the RES2DINV software is divided into horizontal layers with each layer having resistivity values corresponding to the location of the electrodes in the array. The last layer corresponding to the deepest point of the survey and the first layer corresponding to the ground surface area of the survey line, see Figure (6.15) to Figure (6.18).

From Figure (6.15) to Figure (6.18) the first layer is at a depth of 0.938m which is approximately the depth at which the O.T3 soil sample was taken and the depth at which the Decagon 5TE data logger sensor was placed. The resistivity values at point X in the inversion model pseudosection for the first layer for each month is matched with the corresponding temperature and VWC values measured by the data logger, see Table (6.3). From Table (6.3) there is a break in the trend of data in the month of August due to failure in the data logger power source, hence no data was captured.

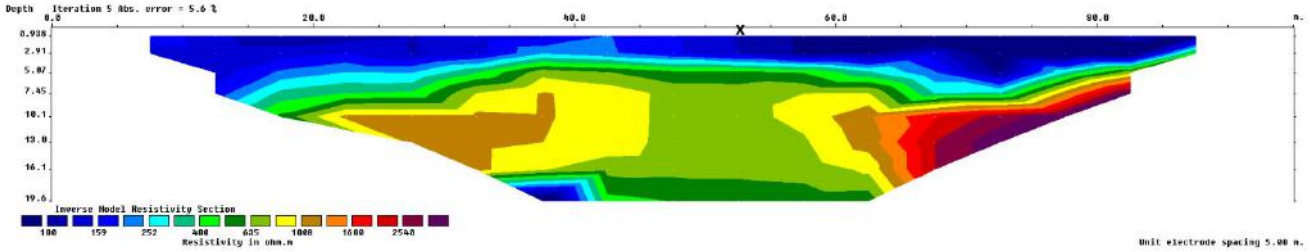

Figure 6.15: Inverse Model Resistivity Section for the month of June.

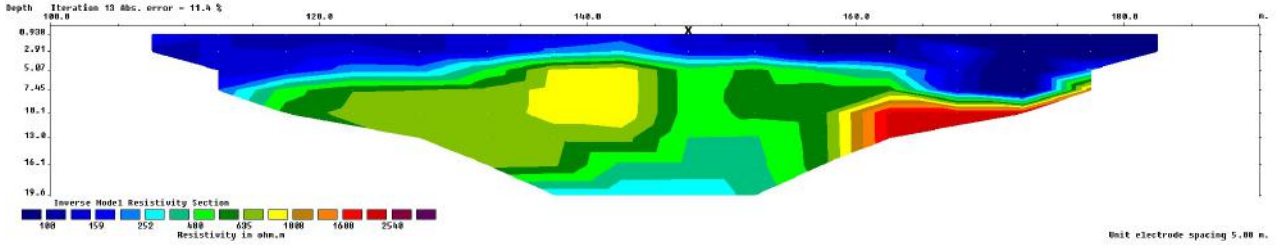

Figure 6.16: Inverse Model Resistivity Section for the month of July.

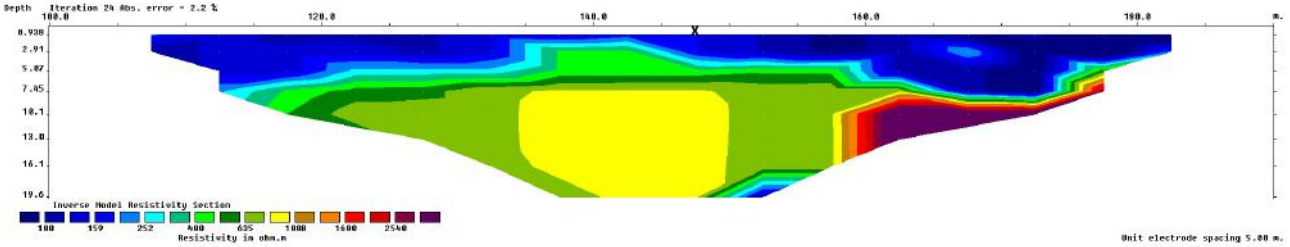

Figure 6.17: Inverse Model Resistivity Section for the month of August.

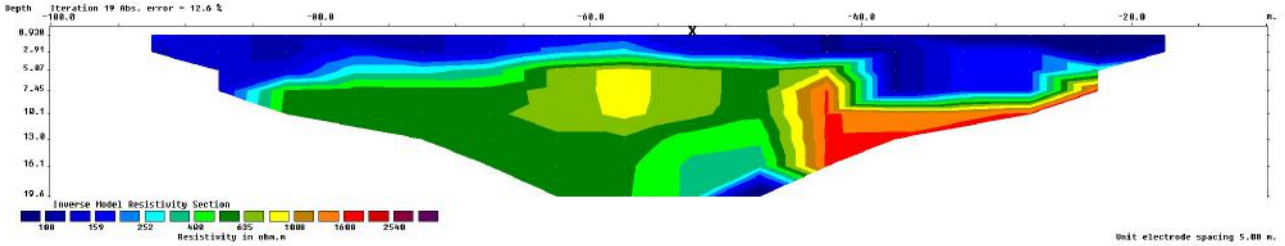

Figure 6.18: Inverse Model Resistivity Section for the month of October.

Table 6.3: O.T3 field resistivity values with corresponding temperature and moisture content

Time	Volumetric water content %	Temperature (°C)	Apparent Resistivity (Ωm)
12.6.2019	25	11	163.84
24.7.2019	24	13	153.93
16.8.2019	20	14	160.16
24.10.2019	37	9	147,08

The apparent resistivity, VWC, and temperature of the O.T3 field data is plotted against time. It can be observed in Figure (6.19) that from the end of July the apparent resistivity and VWC have an inverse correlation whereas the soil temperature has a direct correlation with apparent resistivity. To understand this phenomenon, the resistivity of field saturated soil and resistivity of water ponding at the bottom of the dug-out test pit of the sandy silty Clay soil (O.T3) was measured as described in section 5.3, see Figure (5.11) and Figure (5.12). It is observed that the resistivity of field saturated soil is 151.42 Ωm while the pore water has a resistivity of 70.42 Ωm making the pore water two times more conductive than the soil matrix. Using Eq. (16), the TDS of O.T3 is estimated to be 92mg/l. This means that the pore water works as a channel for electric current since it is has a higher conductivity.

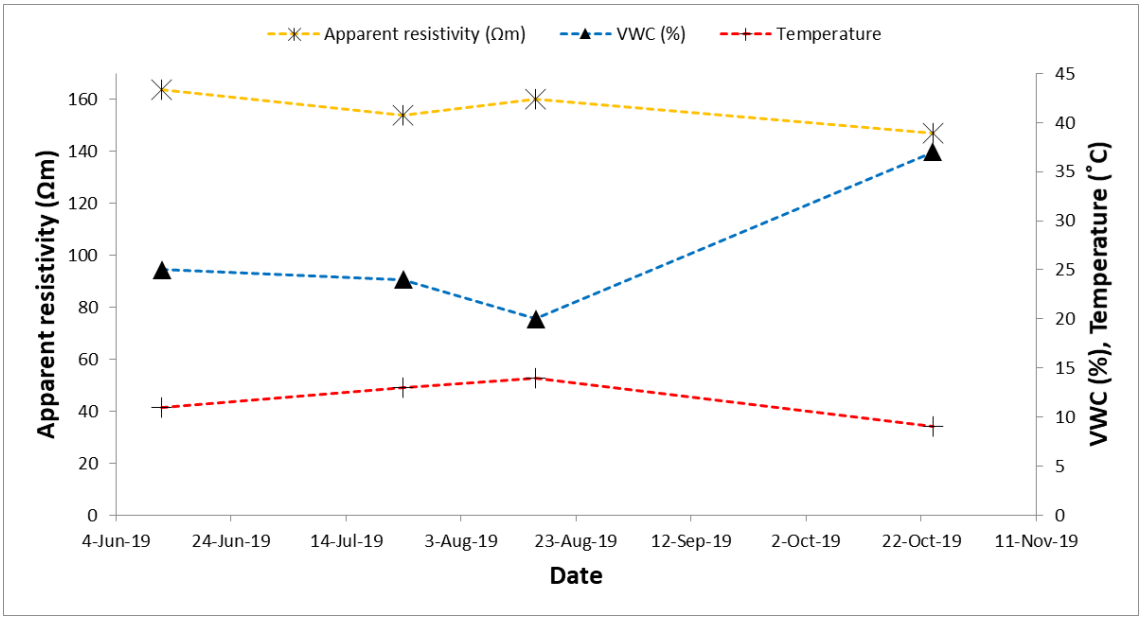

Figure 6.19: Relation between field resistivity, water content, and temperature for O.T3.

Although the O.T3 field data was collected is short period of 5 months, the results above were compared to the results measured 10 years earlier in Metsähovi (Hokkanen, 2011). ERT measurements were carried out with an electrode spacing of

1m from 17 September 2008 to 5 November 2010, see Figure (6.20). The apparent resistivity, VWC, and temperature of the M.H resistivity field data is plotted against time.

This monitoring data involves three periods when soil temperature increased in the subsurface following the warm summer season. The apparent resistivity follows inversely the soil temperature. During the first high temperature period, VWC did not change much. During the subsequent warm periods, VWC shows a minimum. From the relationship, it is observed that the decrease of VWC does not affect apparent resistivity significantly, but the soil temperature has an inverse correlation with apparent resistivity of the silty Clay (siCl) soil, see Figure (6.21). Also, the field saturated soil matrix soil and the pore water of the silty Clay (M.H) was measured by Hokkanen (2011). It was observed that the Metsähovi (M.H) Silty Clay matrix has a resistivity of 17Ωm while the pore water has a resistivity of 250Ωm making the pore water a lot less conductive than the soil matrix.

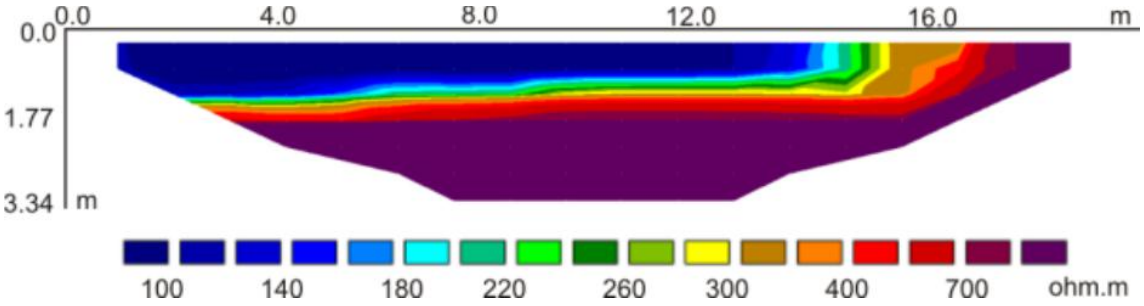

Figure 6.20: Inverse Model Resistivity Section for M.H (Hokkanen, 2011)

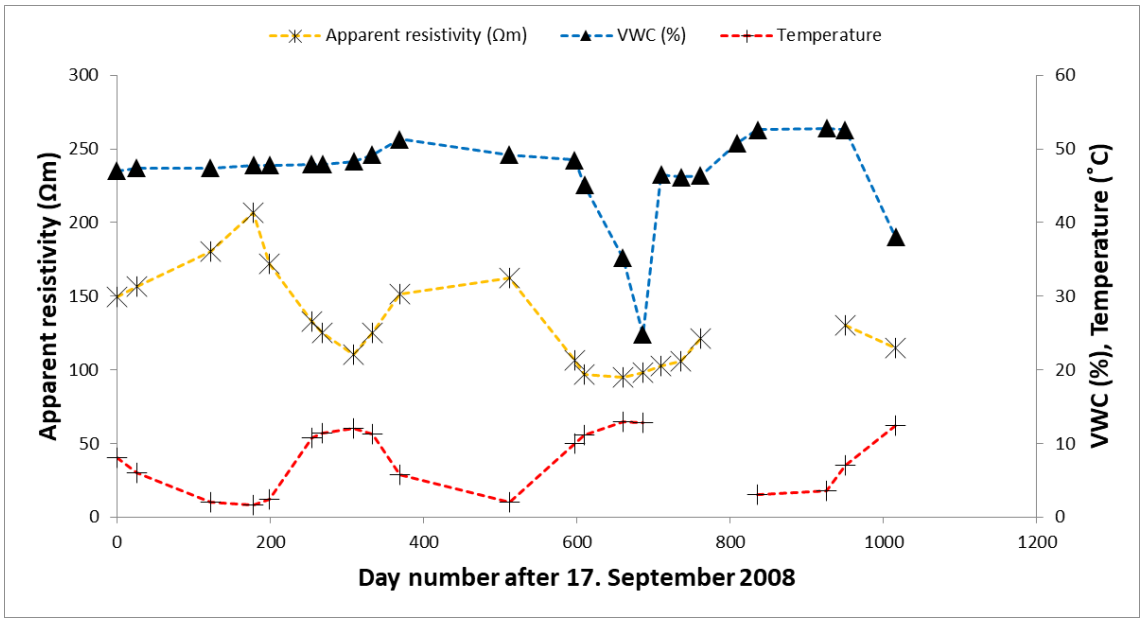

Figure 6.21: Relation between field resistivity, water content, and temperature for M.H. Source: Modified from Hokkanen (2011).

7 Discussions

The results used in the analysis were obtained from samples and field test from two different locations in the study area as seen in Section 3. From these two locations, 5 laboratory and 1 field data represented Otaniemi while 1 laboratory 1 field data are from the Metsähovi area. It can be observed that in the laboratory measurement, the apparent resistivity for all the soil samples is influenced by the temperature of the soil. For each 1°C increase in soil temperature when saturated, there is approximately 2% decrease in apparent resistivity value for the fine grain samples. This relationship has been established by many researchers like Campbell et al. (1948), Samouëlia et al., (2005), Colman and Hendrix (1949), Michot et. Al., (2003). The ERT laboratory results also show a similar relationship to the ERT investigations carried out by Hu et al. (2019) on subgrade soils, see Section 2.1.2. Although the laboratory test conditions by Hu et al. (2019) had soil temperature ranging from 17 to 25 and moisture content levels of 12%, 17%, and 22%, this differs from the test conditions in this study with soil temperature ranging from 2°C to 14°C and moisture content ranging from 10 to 58%. Both results show soil resistivity reduces as the soil moisture and temperature increases.

The ERT laboratory results for the fine grained soil samples (M.H, O.T1, O.T2 O.T3) in this study show that the soil resistivity dependency on temperature reduces significantly at VWC greater than 20% in other words the gradient flattens, see Figure (6.3) to Figure (6.6). Also the results in Figure (6.9) to Figure (6.12) show ERT is significantly influenced by VWC, but the influence is minimal when VWC is above 20%. This observation is consistent with the observation made by Bai et al. (2013) on lateritic soils that the soil resistivity is significantly influenced by water content, but a minor influence is observed when the moisture content is above 23.4%. The similarity to the results of Bai et al. (2013) is evident if the measurements of resistivity are plotted against the water content as in Figures (6.9) - (6.14) are compared to measurements of Bai et al. (2013) given in Figure (2.8). From these observations, the soil temperature effects more on ERT when the moisture content is less than 20% for fine grained soils. Since both M.H sample (Metsähovi area) and O.T3 (Otaniemi area) represent Clay silt from two different areas, their laboratory and field data are compared. A quantitative representative comparison between both sets of data from these two locations is done, see Table (7.1).

From the ERT laboratory test, it is observed that there are 2.7% and 2% decrease in saturated soil resistivity per 1°C increase in temperature for O.T3 and M.H soil samples at 45%, 58% VWC) respectively. Also, the % decrease in apparent resistivity per 1% increase in VWC from unsaturated to saturated VWC at 8°C for O.T3 and M.H soil samples are 4.5% and 3% respectively. The effect of water content on the resistivity of the O.T3 soil sample, when compared to M.H soil sample, is 50% higher. Since both soil samples are clay silt and the resistivity and TDS of the tap water used in the test are the same, it is assumed both should have similar responses. To confirm the cause of this discrepancy, the sensitivity of the soil resistivity to changes in water content is calculated as explained in Section 6.2. O.T3 and M.H soil samples both have a sensitivity of 3.42% and 0.6% respectively, making O.T3 soil sample

approximately 5.5 times more sensitive to change in water content than M.H sample.

The resistivity field results from the (M.H) Clay silty soil show the resistivity of the soil was dependent on soil temperature as seen in Figure (6.21). This can be attributed to the soil water content with a resistivity value of 250Ωm and TDS of 26mg/l being a lot more resistive than the soil matrix with a resistivity value of 17Ωm. In general, sand has a low conductivity, silt has a medium conductivity, and clay has a high conductivity. Consequently, EC correlates strongly to soil particle size and texture. Hence, depending on the matrix of the soil type the ERT measurement would likely be more dependent on the water content or the temperature. M.H has higher clay content (27.7%)compared to OT3 (18.4%). The proportion of silt-sized grains in both samples are about the same 35% and O.T3 has consequently higher sand contents (49%). Therefore, the lower matrix resistivity of M.H compared to O.T3 measured (17Ωm, 51.4Ωm, respectively) can be probably attributed to the higher clay content measured (27.7%, 18.4%, respectively). Refer to cumulative grain-size distribution curves given in Figure (6.1). The O.T3 soil with more sand content and less clay content have a less conductive soil matrix which makes the ERT measurement of this soil type more dependent on water content and/or the EC of pore water.

The ratios of water resistivity in the two sites are opposite to those of soil matrix. In Otaniemi, pore water sample had lower resistivity compared the pore water sample in Metsähovi (70.42Ωm compared to 250Ωm respectively). The present elevation suggests that clays sampled and monitored in Metsähovi have been deposited in the Yoldia or Anculys stage of the Baltic Sea basin, see Section 3. During these stages, the salinity of the basin water has been lower(fresh or only mildly brackish) than the present Baltic seawater. The field investigation and sampling site in Otaniemi likely represents Litorina or present Baltic sea deposits. During the Litorina stage seawater has been more saline that the present Baltic seawater. According to Gardemaister (1975), the evolution of the Baltic basin water is reflected also in the pore water salinity of the fine deposits in Finland. After the conversion of measured resistivity to EC and water salinity, the measured values can be found to be consistent with observations by Gardemeister.

What was interesting to note is that the tap water has lower resistivity (52Ωm) than the pore water resistivities of O.T3 and M.H (70.42Ωm, 250Ωm respectively). Comparing O.T3 VWC for both laboratory and field measurements, it is observed that the minimum VWC in the field is 20% and the maximum is 37%. This VWC level is when soil resistivity dependency on temperature reduces significantly and hence the temperature dependency is not observed. While the minimum VWC in the laboratory measurement is 10% and the maximum is 45% and the soil resistivity dependency on temperature is observed when VWC is less than 20%, see Figure (6.6). When the same comparison is made for M.H, it is observed that in the field measurement even at the highest and lowest VWC (53% 25% respectively) the soil resistivity was dependent on the soil temperature, see Figure (6.21). At these VWC soil resistivity dependency on temperature should significantly reduce but it does not in this case. This could be attributed to the M.H soil matrix having a low resistivity of 172Ωm (high EC) due to the TDS from the Yoldia sea.

Table 7.1: Comparison between O.T3 and M.H ERT field and laboratory results

Field test	**O.T3**			**M.H**		
	Minimum	**Maximum**	**Median**	**Minimum**	**Maximum**	**Median**
Temperature (°C)	9	14	12	2	13	8
VWC (%)	20	37	25	25	53	48
Resistivity (Ωm)	147.08	163.84	157	95	207	125
Pore water resistivity (Ωm)	70.42			250		
TDS in pore water (mg/l)	92			26		
Soil matrix resistivity (Ωm)	51.42			17		
Duration of field observation	June 2019 to October 2019			September 2008 to November 2010		
Laboratory test						
	Minimum	**Maximum**	**Median**	**Minimum**	**Maximum**	**Median**
Temperature (°C)	2	14	8	2	14	8
VWC (%)	10	45	25	11	58	33
Tap water resistivity (Ωm)	52			52		
TDS in tap water (mg/l)	125			125		
% of Clay content (<0.063 mm)	18.41			27.19		
% of sand content (0.063mm - 2mm)	49.06			11.26		
% decrease in saturated soil resistivity per 1°C increase in temperature	2.75%			2%		
Resistivity % decrease per 1% VWC increase from unsaturated to saturated soil	4.5%			3%		
Sensitivity to change in VWC (%)	3.42%			0.62%		

8 Conclusions

The ERT laboratory measurement shows that the apparent resistivity for all the soil samples is influenced by the temperature of the soil. Also from the laboratory results, it can be seen that the apparent resistivity of the different soil types is also influenced by the soil water content. As the water content was increased, the resistivity of the soil decreased which means as the soil gets saturated the resistivity of the soil decreases.

In both controlled ERT laboratory conditions and Field ERT measurements, some Clay silt samples are sensitive to the change in water content, but some are not. This could be attributed to the TDS in the soil and pore water. M.H pore water has a low TDS and a highly conductive soil matrix with higher clay content and less sand. The results show that laboratory test differs from the field results in the sense that the field ERT is dependent on soil temperature, while the laboratory ERT is dependent more on VWC. This attribute can be as a result of the clay silt structure being disturbed and the composition of pore water can vary a lot from the origin of the formation of the soil. While clay silt soil with more sand content and less clay content which in this case the O.T3 Clay silt have a less conductive soil matrix which makes the ERT measurement of this soil type more dependent on water content. For these reasons, precaution must be taken when using ERT for engineering works, water content monitoring during different seasons and the temperature of the soil must be considered, if not errors in interpretation may occur.

References

ABEM, A. I. 2009. *Terrameter SAS1000/4000 LUND Imaging System Introduction Manual.*

Alalammi, P., Eklund, C., Hakli Gillian. (1992). *Suomen kartasto / Atlas over Finland / utgivare: Lantmateristyrelsen, Geografiska sallskapet i Finland = Atlas of Finland / publishers: National Board of Survey, Geographical Society of Finland.* Helsinki: Maanmittaushallitus.

Bai, W., Kong, L., Guo, A. (2013). Effects of Physical Properties on Electrical Conductivity of Compacted Lateritic Soil. *Journal of Rock Mechanics and Geotechnical Engineering,* vol. 5, no. 5, 2013, pp. 406–411., doi:10.1016/j.jrmge.2013.07.003.

Bell, F., G. (2007). Basic Environmental and Engineering Geology. *Whittles Publishing,* pp. 225.

Campbell, R. B., Bower, C. A., Richards, L. A. (1949). Change of Electrical Conductivity With Temperature and the Relation of Osmotic Pressure to Electrical Conductivity and Ion Concentration for Soil Extracts. *Soil Science Society of America Journal,* vol. 13, no. C, 1949, pp. 66–69. doi: 10.2136/sssaj1949.036159950013000c0010x

Colman, E. A., Hendrix, T. M. (1949). The Fiberglass Electrical Soil-Moisture Instrument. *Soil Science,* vol. 67, no. 6, 1949, pp. 425–438. doi: 10.1097/00010694-194906000-00002

Craig, R. F. (2004). *Craig's Soil Mechanics (7th ed.).* London: Spon Press - Taylor Francis Group.

Das, B., M. (2010). Principles of Geotechnical Engineering. *Seventh ed., Cengage Learning,* pp. 15–104.

Green, T. R., Taniguchi, M., Kooi, H., Gurdak, J., Allen, D. M., Hiscock, K. M., Treidel, H., Aureli, A. (2011). Beneath the Surface of Global Change: Impacts of Climate Change on Groundwater. *Journal of Hydrology,* vol. 405, no. 3-4, 2011, pp. 532–560. doi: 10.1016/j.jhydrol.2011.05.002

Gardemeister, R. (1975). *On Engineering-Geological Properties of Fine-Grained Sediments in Finland.* Valtion Teknillinen Tutkimuskeskus.

Hayley, K., Bentley, L. R., and Pidlisecky, A. (2010). Compensating for temperature variations in time-lapse electrical resistivity difference imaging. *Geophysics,* 2010, vol. 75, nro 4, s. WA51-WA59. doi: 10.1190/1.3478208

Hauck, C. (2002). Frozen Ground Monitoring Using DC Resistivity Tomography. *Geophysical Research Letters,* vol. 29, nro 21, s. 12-1-12-4. doi: 10.1029/2002gl014995

Hayashi, M. (2004). Temperature-Electrical Conductivity Relation of Water for Environmental Monitoring and Geophysical Data Inversion. *Environmental Monitoring and Assessment,* vol. 96, no. 1-3, 2004, pp. 119–128., doi:10.1023/b:emas.0000031719.83065.68.

Herman, R. (2001). An Introduction to Electrical Resistivity in Geophysics. *American Journal of Physics,* vol. 69, no. 9, pp. 943–952.

Hermans, T., Vandenbohede, A., Lebbe, L., Nguyen, F. (2012). A Shallow Geothermal Experiment in a Sandy Aquifer Monitored Using Electric Resistivity Tomography. *Geophysics,* vol. 77, no. 1, s. B11-B21.

Hokkanen, T. (2016). Gravity Effects of Local Soil Moisture and Groundwater Fluctuations to the Superconducting Gravimeter at Metsähovi, Finland. Retrieved from https://aaltodoc.aalto.fi/handle/123456789/23706

Hokkanen, T. (2011). Maankamaran lämpötilan ja kosteuden vaikutus maavastusluotauksiin Metsähovin tutkimusalueella. *Sovelletun Geofysiikan XVIII Neuvottelupäivät,* Otaniemi 2011. Otaniemi 2011, Vuorimiesyhdistys.

Hu, Z., Peng, K., Li, L., Ma, Q., Xiao, H., Li, Z., Ai, P. (2019). Effect of Wetting-Drying Cycles on Mechanical Behaviour and Electrical Resistivity of Unsaturated Subgrade Soil. *Advances in Civil Engineering,* vol. 2019, 2019, pp. 1–10., doi:10.1155/2019/3465327.

Korhonen, K. H, Gardemeister, R., Tammirinne, M. (1974). *Geotekninen Maaluokitus.* Otaniemi: Valtion Teknillinen Tutkimuskeskus.

Loke, M., H. (2011). Tutorial: 2-D and 3-D Electrical Imaging Survey Manual.

McDowell, P. W., Barker, R. D., Butcher, A. P., Culshaw, M. G., Jackson, P. D., McCann, D. M., Skipp, B. O., Matthews, S. L. Arthur, J. C. R. (2002). *Geophysics in Engineering Investigations.* CIRIA.

Merritt, A. 4D Geophysical Monitoring of Hydrogeological Precursors to Landslide Activation. *White Rose ETheses Online,* University of Leeds, 1 Apr. 2014, http://etheses.whiterose.ac.uk/7422/.

Michot, D., Benderitter, Y., Dorigny, A., Nicoullaud, B., King, D., Tabbagh A. (2003). Spatial and Temporal Monitoring of Soil Water Content with an Irrigated Corn Crop Cover Using Surface Electrical Resistivity Tomography. *Water Resources Research,* 2003, vol. 39, no. 5, s. 14-1-14-19. doi: 10.1029/2002wr001581

Mitchell, J., Soga, K. (2013).*Fundamentals of Soil Behavior.* John Wiley Sons, pp. 173–193.

Mostafa, M.S., Afify, N., Abozid, E. F., and Gaber, A. (2003). Electrical Resistivity of Some Basalt and Granite Samples From Egypt *Egypt. J. Sol,* vol. 26, nro 1, s. 25-32.

Ojala, Antti, E. K., Saresma, M., Virtasalo, J, Huotari-Halkosaari, T. (2016). An Allostratigraphic Approach to Subdivide Fine-Grained Sediments for Urban Planning. *Bulletin of Engineering Geology and the Environment,* vol. 77, no. 2, 2016, pp. 879–892. doi: 10.1007/s10064-016-0981-4

Okkonen, J. (2011). Groundwater and Its Response to Climate Variability and Change in Cold Snow Dominated Regions in Finland: Methods and Estimations. *CORE,* Oulun Yliopisto, https://core.ac.uk/display/71807185.

Palacky, G. J. (1988). Resistivity Characteristics of Geologic Targets. *Electromagnetic Methods in Apllied Geophysics,* pp. 53–129. doi: 10.1190/1.9781560802631.ch3

Rein, A., Hoffmann, R., and Dietrich, P. (2004) .Influence of Natural Time-Dependent Variations of Electrical Conductivity on DC Resistivity Measurements. *Journal of Hydrology,* vol. 285, s. 215-232.

Reynolds, J. M. (1997). *An Introduction to Applied and Environmental Geophysics.* John Wiley Sons Ltd, Baffins Lane, Chichester, West Sussex POl9 IUD, England.

Samouëlian, A., Cousin, I., Tabbagh, A., Bruand, A., Richard, G. (2005). Electrical Resistivity Survey in Soil Science: a Review. *Soil and Tillage Research,* vol. 83, no. 2, pp. 173–193.

Schlumberger Log Interpretation Charts. https://www.scribd.com/doc/95998488/Schlumberger-Log-Interpretation-Chart

ClimateElements. Finnish Meteorological Institute, https://en.ilmatieteenlaitos.fi/climate-elements

SFS-EN ISO 14688-1:en (2018). Geotechnical investigation and testing. Identification and classification of soil. Part 1: Identification and description, Finnish Standards Association SFS, Helsinki.

SFS-EN ISO 14688-2:en (2018). Geotechnical investigation and testing. Identification and classification of soil. Part 2: Principles for a classification, Finnish Standards Association SFS, Helsinki.

Telford, W. M., Geldart, L. P., Sheriff, R., E. (2010). *Applied Geophysics.* Cambridge Univ. Press.

Appendix A Sieving and Hydrometer Test Report

Table A1: M.H Sample

Diameter	Soil Retained		Cumulative	Soil Passing	
mm	g	%	%	g	%
64	0	0,00 %	0,00 %	50	100,00 %
32	0	0,00 %	0,00 %	50	100,00 %
16	0	0,00 %	0,00 %	50	100,00 %
8	0	0,00 %	0,00 %	50	100,00 %
4	0	0,00 %	0,00 %	50	100,00 %
2	0	0,00 %	0,00 %	50	100,00 %
1	0,62	1,24 %	1,24 %	49,38	98,76 %
0,5	0,75	1,50 %	2,74 %	48,63	97,26 %
0,25	0,76	1,52 %	4,26 %	47,87	95,74 %
0,125	1,93	3,86 %	8,12 %	45,94	91,88 %
0,063	1,57	3,14 %	11,26 %	44,37	88,74 %
Pan	44,37	88,74 %	100,00 %	0	0,00 %
Sum	50	100,00 %			

Particle density (g/cm)	2,67	Dry sample (g)	50
Sludge Quantity (cc)	1000	Hydrometer calibration in dZ / dR	265
Dry sample (g)	50	Hydrometer correction	-0,0016

D85	D60	D50	D10	Savi %	Hieno % (<0,063mm)
0 mm	0 mm	0 mm	0 mm	27,2 %	88,7 %

Diameter	Passing	k	b	85,00 %
64	1,00			0,04 mm
32	1,00	0	1	60,00 %
16	1,00	0	1	0,01 mm
8	1,00	0	1	50,00 %
4	1,00	0	1	0,01 mm
2	1,00	0	1	10,00 %
1	0,99	0,0124	0,975	0,00 mm
0,5	0,97	0,03	0,958	
0,25	0,96	0,0608	0,942	
0,125	0,92	0,3088	0,88	Gravel content
0,063	0,89	0,5065	0,855	63 - 2 mm
0,0347	0,83	2,0359	0,759	0,00 %
0,0148	0,74	4,4903	0,674	Sand content
0,0097	0,65	17,417	0,482	2 - 0,063
0,0057	0,53	30,313	0,357	11,26 %
0,0028	0,35	61,863	0,177	Fines content
0,0012	0,20	98,593	0,075	0,063
0,0006	0,13	114,94	0,054	88,74 %
0,0006	0,11	200,38	-0	Clay content
0,0006	0,11	-44,07	0,14	0,002
0,0006	0,09	505,91	-0,22	27,19 %

Time			Time	Temperature	Water density	Water Viscosity	Hydrometer reading		Zr		Penetration	Penetration Incorporated
h	m	s	s	C	g/cm	g.s/cm			cm		%	%
After the hydrometer screening (# 0.063mm coarser mass) is used for screening and hydrometer combination										0,06300	88,74 %	88,74 %
	1	17	77	25	0,9970525	9,12995E-06	1,0264	1,0248	9,464	0,03475	82,99 %	82,99 %
	7	35	455	25	0,9970525	9,12995E-06	1,0236	1,022	10,206	0,01484	74,05 %	74,05 %
	19		1140	25	0,9970525	9,12995E-06	1,0208	1,0192	10,948	0,00971	65,11 %	65,11 %
1			3600	25	0,9970525	9,12995E-06	1,0170	1,0154	11,955	0,00571	52,98 %	52,98 %
4	45	52	17152	25,2	0,9970024	9,08799E-06	1,0113	1,0097	13,4655	0,00277	34,79 %	34,79 %
25	43	50	92630	25	0,9970525	9,12995E-06	1,0066	1,005	14,711	0,00125	19,79 %	19,79 %
100	37	10	362230	25,8	0,9968497	8,96373E-06	1,0044	1,0028	15,294	0,00064	12,77 %	12,77 %
120			432000	27,6	0,99637	8,60478E-06	1,0040	1,0024	15,4	0,00057	11,49 %	11,49 %
100	37	10	362230	25	0,9970525	9,12995E-06	1,0039	1,0023	15,4265	0,00065	11,17 %	11,17 %
120			432000	25	0,9970525	9,12995E-06	1,0031	1,0015	15,6385	0,00060	8,62 %	8,62 %

Table A2: O.T1 Sample

Diameter	Soil Retained		Cumulative	Soil Passing	
mm	g	%	%	g	%
64	0	0,00 %	0,00 %	50	100,00 %
32	0	0,00 %	0,00 %	50	100,00 %
16	0	0,00 %	0,00 %	50	100,00 %
8	0	0,00 %	0,00 %	50	100,00 %
4	0	0,00 %	0,00 %	50	100,00 %
2	0,49	0,98 %	0,98 %	49,51	99,02 %
1	0,21	0,42 %	1,40 %	49,3	98,60 %
0,5	0,49	0,98 %	2,38 %	48,81	97,62 %
0,25	0,74	1,48 %	3,86 %	48,07	96,14 %
0,125	1,75	3,50 %	7,36 %	46,32	92,64 %
0,063	10,37	20,74 %	28,10 %	35,95	71,90 %
Pan	35,95	71,90 %	100,00 %	0	0,00 %
Sum	50	100,00 %			

Particle density (g/cm)	2,68	Dry sample (g)	50
Sludge Quantity (cc)	1000	Hydrometer calibration in dZ / dR	265
Dry sample (g)	50	Hydrometer correction	-0,0016

D85	D60	D50	D10	Savi %	Hieno % (<0,063mm)
0,1 mm	0 mm	0 mm	0 mm	21,9 %	71,9 %

Diameter	Passing	k	b	85,00 %
64	1,00			0,10 mm
32	1,00	0	1	60,00 %
16	1,00	0	1	0,04 mm
8	1,00	0	1	50,00 %
4	1,00	0	1	0,03 mm
2	0,99	0,0049	0,98	10,00 %
1	0,99	0,0042	0,982	#DIV/0!
0,5	0,98	0,0196	0,966	
0,25	0,96	0,0592	0,947	
0,125	0,93	0,28	0,891	Gravel content
0,063	0,72	3,3452	0,508	63 - 2 mm
0,0353	0,54	6,405	0,315	0,98 %
0,0186	0,43	6,4934	0,312	Sand content
0,0105	0,37	7,8503	0,287	2 - 0,063
0,0061	0,32	11,005	0,254	27,12 %
0,0028	0,25	22,878	0,181	Fines content
0,0012	0,19	32,697	0,154	0,063
0,0006	0,16	51,927	0,13	71,90 %
0,0006	0,13	477,7	-0,14	Clay content
0,0006	0,16	477,7	-0,14	0,002
0,0006	0,13	477,7	-0,14	21,90 %

Time			Time	Temperature	Water density	Water Viscosity	Hydrometer reading		Zr		Penetration	Penetration Incorporated
h	m	s	s	C	g/cm	g.s/cm			cm		%	%
After the hydrometer screening (# 0.063mm coarser mass) is used for screening and hydrometer combination										0,06300	71,90 %	71,90 %
	1	33	93	25	0,9970525	9,12995E-06	1,0174	1,0158	11,849	0,03527	54,14 %	54,14 %
	6		360	25	0,9970525	9,12995E-06	1,0140	1,0124	12,75	0,01860	43,31 %	43,31 %
	19	40	1180	25	0,9970525	9,12995E-06	1,0120	1,0104	13,28	0,01048	36,94 %	36,94 %
	59		3540	25	0,9970525	9,12995E-06	1,0105	1,0089	13,6775	0,00614	32,17 %	32,17 %
4	55	27	17727	25,2	0,9970024	9,08799E-06	1,0081	1,0065	14,3135	0,00280	24,52 %	24,52 %
25	52	22	93142	25	0,9970525	9,12995E-06	1,0065	1,0049	14,7375	0,00124	19,43 %	19,43 %
100	44	46	362686	25,8	0,9968497	8,96373E-06	1,0055	1,0039	15,0025	0,00063	16,24 %	16,24 %
120			432000	27,6	0,99637	8,60478E-06	1,0046	1,003	15,241	0,00057	13,38 %	13,38 %
100	44	46	362686	25,8	0,9968497	8,96373E-06	1,0055	1,0039	15,0025	0,00063	16,24 %	16,24 %
120			432000	27,6	0,99637	8,60478E-06	1,0046	1,003	15,241	0,00057	13,38 %	13,38 %

Table A3: O.T2 Sample

Diameter	Soil Retained		Cumulative	Soil Passing	
mm	g	%	%	g	%
64	0	0,00 %	0,00 %	50	100,00 %
32	0	0,00 %	0,00 %	50	100,00 %
16	0	0,00 %	0,00 %	50	100,00 %
8	0	0,00 %	0,00 %	50	100,00 %
4	0	0,00 %	0,00 %	50	100,00 %
2	0	0,00 %	0,00 %	50	100,00 %
1	0,48	0,96 %	0,96 %	49,52	99,04 %
0,5	0,59	1,18 %	2,14 %	48,93	97,86 %
0,25	2,04	4,08 %	6,22 %	46,89	93,78 %
0,125	5,38	10,76 %	16,98 %	41,51	83,02 %
0,063	3,56	7,12 %	24,10 %	37,95	75,90 %
Pan	37,86	75,72 %	99,82 %	0,09	0,18 %
Sum	50	99,82 %			

Particle density (g/cm)	2,67	Dry sample (g)	50
Sludge Quantity (cc)	1000	Hydrometer calibration in dZ / dR	265
Dry sample (g)	50	Hydrometer correction	-0,0016

D85	D60	D50	D10	Savi %	Hieno % (<0,063mm)
0,1 mm	0 mm	0 mm	0 mm	38,3 %	75,9 %

Diameter	Passing	k	b	85,00 %
64	1,00			0,15 mm
32	1,00	0	1	60,00 %
16	1,00	0	1	0,01 mm
8	1,00	0	1	50,00 %
4	1,00	0	1	0,00 mm
2	1,00	0	1	10,00 %
1	0,99	0,0096	0,981	0,00 mm
0,5	0,98	0,0236	0,967	
0,25	0,94	0,1632	0,897	
0,125	0,83	0,8608	0,723	Gravel content
0,063	0,76	1,1484	0,687	63 - 2 mm
0,0410	0,73	1,2779	0,678	0,00 %
0,0186	0,70	1,4218	0,673	Sand content
0,0103	0,64	7,7316	0,555	2 - 0,063
0,0058	0,55	19,848	0,43	24,10 %
0,0026	0,43	35,969	0,336	Fines content
0,0012	0,32	75,848	0,231	0,063
0,0006	0,23	164,63	0,124	75,90 %
0,0006	0,17	1136,7	-0,48	Clay content
0,0006	0,11	-749,9	0,596	0,002
0,0006	0,09	509,93	-0,22	38,29 %

Time			Time	Temperature	Water density	Water Viscosity	Hydrometer reading		Zr	Penetration	Penetration Incorporated
h	m	s	s	C	g/cm	g.s/cm			cm	%	%
After the hydrometer screening (# 0.063mm coarser mass) is used for screening and hydrometer combination									0,06300	75,90 %	75,90 %
	1		60	25	0,9970525	9,12995E-06	1,0233	1,0217	10,2855	0,04104	73,09 %	73,09 %
	5		300	25	0,9970525	9,12995E-06	1,0223	1,0207	10,5505	0,01859	69,90 %	69,90 %
	17		1020	25	0,9970525	9,12995E-06	1,0203	1,0187	11,0805	0,01033	63,52 %	63,52 %
1	3	48	3420	25	0,9970525	9,12995E-06	1,0175	1,0159	11,8225	0,00583	54,58 %	54,58 %
4	55	7	17940	25,4	0,9969519	9,0463E-06	1,0139	1,0123	12,7765	0,00263	43,09 %	43,09 %
25	49	14	93000	25	0,9970525	9,12995E-06	1,0105	1,0089	13,6775	0,00120	32,24 %	32,24 %
100	44	37	362677	25,8	0,9968497	8,96373E-06	1,0075	1,0059	14,4725	0,00062	22,66 %	22,66 %
120			432000	27	0,9965335	8,72222E-06	1,0057	1,0041	14,9495	0,00057	16,92 %	16,92 %
100	44	37	362677	25	0,9970525	9,12995E-06	1,0039	1,0023	15,4265	0,00065	11,17 %	11,17 %
120			432000	25	0,9970525	9,12995E-06	1,0031	1,0015	15,6385	0,00060	8,62 %	8,62 %

Table A4: O.T3 Sample

Diameter	Soil Retained		Cumulative	Soil Passing	
mm	g	%	%	g	%
64	0	0.00%	0.00%	50	100.00%
32	0	0.00%	0.00%	50	100.00%
16	0	0.00%	0.00%	50	100.00%
8	0	0.00%	0.00%	50	100.00%
4	0	0.00%	0.00%	50	100.00%
2	0	0.00%	0.00%	50	100.00%
1	1.45	2.90%	2.90%	48.55	97.10%
0.5	2.02	4.04%	6.94%	46.53	93.06%
0.25	4.67	9.34%	16.28%	41.86	83.72%
0.125	8.87	17.74%	34.02%	32.99	65.98%
0.063	7.52	15.04%	49.06%	25.47	50.94%
Pan	25.02	50.04%	99.10%	0.45	0.90%
Sum	50	99.10%			

Particle density (g/cm)	2.65	Dry sample (g)	50
Sludge Quantity (cc)	1000	Hydrometer calibration in dZ / dR	265
Dry sample (g)	50	Hydrometer correction	-0,0016

D85	D60	D50	D10	Savi %	Hieno % (<0,063mm)
0.3 mm	0.1 mm	0.1 mm	0 mm	18.4 %	50.9 %

Diameter	Passing	k	b	85,00 %
64	1.00			0.28 mm
32	1.00	0	1	60,00 %
16	1.00	0	1	0.10 mm
8	1.00	0	1	50,00 %
4	1.00	0	1	0.06 mm
2	1.00	0	1	10,00 %
1	0.97	0.029	0.942	0,00 mm
0.5	0.93	0.0808	0.89	
0.25	0.84	0.3736	0.744	
0.125	0.66	1.4192	0.482	Gravel content
0.063	0.51	2.4258	0.357	63 - 2 mm
0.0458	0.45	3.6976	0.276	0,00 %
0.0208	0.39	2.0553	0.352	Sand content
0.0112	0.33	6.6651	0.256	2 - 0,063
0.0060	0.28	9.956	0.219	49.06%
0.0029	0.21	21.154	0.151	Fines content
0.0013	0.16	32.417	0.119	0,063
0.0006	0.14	25.573	0.128	50.94%
0.0006	0.09	859.84	-0.41	Clay content
0.0006	0.14	809.37	-0.38	0,002
0.0006	0.09	1120.5	-0.58	18.41%

Time			Time	Temperature	Water density	Water Viscosity	Hydrometer reading		Zr	Penetration	Penetration Incorporated
h	m	s	s	C	g/cm	g.s/cm			cm	%	%
After the hydrometer screening (# 0.063mm coarser mass) is used for screening and hydrometer combination									0.06300	50.94%	50.94%
	1		60	25.1	0.9970275	9.10894E-06	1.0143	1.0127	12.6705	0.04577	44.57%	44.57%
	5		300	25.1	0.9970275	9.10894E-06	1.0127	1.0111	13.0945	0.02081	39.44%	39.44%
	18		1080	25.1	0.9970275	9.10894E-06	1.0107	1.0091	13.6245	0.01119	33.03%	33.03%
1	3	48	3828	25.1	0.9970275	9.10894E-06	1.0091	1.0075	14.0485	0.00603	27.90%	27.90%
4	55	7	17707	25.4	0.9969519	9.0463E-06	1.0070	1.0054	14.605	0.00285	21.16%	21.16%
25	49	14	92954	25	0.9970525	9.12995E-06	1.0054	1.0038	15.029	0.00127	16.03%	16.03%
100	44	37	362677	25.5	0.9969265	9.02556E-06	1.0049	1.0033	15.1615	0.00064	14.43%	14.43%
120			432000	27.6	0.99637	8.60478E-06	1.0033	1.0017	15.5855	0.00058	9.30%	9.30%
100	44	37	362677	25	0.9970525	9.12995E-06	1.0049	1.0033	15.1615	0.00064	14.43%	14.43%
120			432000	25	0.9970525	9.12995E-06	1.0033	1.0017	15.5855	0.00060	9.30%	9.30%

Table A5: T.T1 Sample

Diameter	Soil Retained		Cumulative	Soil Passing	
mm	g	%	%	g	%
64	0	0.00%	0.00%	2267.6	100.00%
32	0	0.00%	0.00%	2267.6	100.00%
16	0	0.00%	0.00%	2267.6	100.00%
8	0	0.00%	0.00%	2267.6	100.00%
4	513.9	22.66%	22.66%	1753.7	77.34%
2	137.1	6.05%	28.71%	1616.6	71.29%
1	151.1	6.66%	35.37%	1465.5	64.63%
0.5	207.3	9.14%	44.51%	1258.2	55.49%
0.25	273.4	12.06%	56.57%	984.8	43.43%
0.125	0	0.00%	56.57%	984.8	43.43%
0.063	531.8	23.45%	80.02%	453	19.98%
Pan	453	19.98%	100.00%	0	0.00%
Sum	2267.6	100.00%			

Particle density (g/cm)	2.65	Dry sample (g)	50		
Sludge Quantity (cc)	1000	Hydrometer calibration in dZ / dR	265		
Dry sample (g)	50	Hydrometer correction	-0,0016		

D85	D60	D50	D10	Savi %	Hieno % (<0,063mm)
5.4 mm	0.7 mm	0.4 mm	0	0	20 %

Diameter	Passing	k	b	85,00 %
64	1.00			5.35 mm
32	1.00	0	1	60,00 %
16	1.00	0	1	0.75 mm
8	1.00	0	1	50,00 %
4	0.77	0.0567	0.547	0.39 mm
2	0.71	0.0302	0.652	10,00 %
1	0.65	0.0666	0.58	0,00 mm
0.5	0.55	0.1828	0.463	
0.25	0.43	0.4823	0.314	
0.25	0.43	0	0.434	Gravel content
0.063	0.20	1.2541	0.121	63 - 2 mm
				28.71%
				Sand content
				51.31%
				49.06%
				Fines content
				0,063
				19.98%
				Clay content
				0,002
				0

Time			Time	Temperature	Water density	Water Viscosity	Hydrometer reading	Zr		Penetration	Penetration Incorporated
h	m	s	s	C	g/cm	g.s/cm		cm		%	%
After the hydrometer screening (# 0.063mm coarser mass) is used for screening and hydrometer combination									0.06300	50.94%	50.94%
				25	0.9970525	9.12995E-06		1.0127	12.6705	0.04577	44.57%	44.57%
				25	0.9970525	9.12995E-06		1.0111	13.0945	0.02081	39.44%	39.44%
				25	0.9970525	9.12995E-06		1.0091	13.6245	0.01119	33.03%	33.03%
				25	0.9970525	9.12995E-06		1.0075	14.0485	0.00603	27.90%	27.90%
				25	0.9970525	9.12995E-06		1.0054	14.605	0.00285	21.16%	21.16%
				25	0.9970525	9.12995E-06		1.0038	15.029	0.00127	16.03%	16.03%
				25	0.9970525	9.12995E-06		1.0033	15.1615	0.00064	14.43%	14.43%
				25	0.9970525	9.12995E-06		1.0017	15.5855	0.00058	9.30%	9.30%
				25	0.9970525	9.12995E-06		1.0033	15.1615	0.00064	14.43%	14.43%
				25	0.9970525	9.12995E-06		1.0017	15.5855	0.00060	9.30%	9.30%

Table A6: T.T2 Sample

Diameter	Soil Retained		Cumulative	Soil Passing	
mm	g	%	%	g	%
64	0	0.00%	0.00%	2090	100.00%
32	0	0.00%	0.00%	2090	100.00%
16	0	0.00%	0.00%	2090	100.00%
8	0	0.00%	0.00%	2090	100.00%
4	736.5	35.24%	35.24%	1353.5	64.76%
2	216.2	10.34%	45.58%	1137.3	54.42%
1	216.2	10.34%	55.93%	921.1	44.07%
0.5	283.5	13.56%	69.49%	637.6	30.51%
0.25	317.3	15.18%	84.67%	320.3	15.33%
0.125	0	0.00%	84.67%	320.3	15.33%
0.063	241.9	11.57%	96.25%	78.4	3.75%
Pan	78.4	3.75%	100.00%	0	0.00%
Sum	2090	100.00%			

Particle density (g/cm)	2.78	Dry sample (g)	50		
Sludge Quantity (cc)	1000	Hydrometer calibration in dZ / dR	265		
Dry sample (g)	50	Hydrometer correction	-0,0016		

D85	D60	D50	D10	Savi %	Hieno % (<0,063mm)
6.3 mm	3.1 mm	1.6 mm	0.2 mm	0	3.8 %

Diameter	Passing	k	b	85,00 %
64	1.00			6.30 mm
32	1.00	0	1	60,00 %
16	1.00	0	1	3.08 mm
8	1.00	0	1	50,00 %
4	0.65	0.0881	0.295	1.57 mm
2	0.54	0.0517	0.441	10,00 %
1	0.44	0.1034	0.337	0.16 mm
0.5	0.31	0.2713	0.169	
0.25	0.15	0.6073	0.001	
0.25	0.15	0	0.153	Gravel content
0.063	0.04	0.6189	-0	63 - 2 mm
				45.58%
				Sand content
				2 - 0,063 mm
				50.67%
				Fines content
				0,063
				3.75%
				Clay content
				0,002
				0

Time			Time	Temperature	Water density	Water Viscosity	Hydrometer reading	Zr		Penetration	Penetration Incorporated
h	m	s	s	C	g/cm	g.s/cm		cm		%	%
After the hydrometer screening (# 0.063mm coarser mass) is used for screening and hydrometer combination									0.06300	50.94%	50.94%
				25	0.9970525	9.12995E-06		1.0127	12.6705	0.04577	44.57%	44.57%
				25	0.9970525	9.12995E-06		1.0111	13.0945	0.02081	39.44%	39.44%
				25	0.9970525	9.12995E-06		1.0091	13.6245	0.01119	33.03%	33.03%
				25	0.9970525	9.12995E-06		1.0075	14.0485	0.00603	27.90%	27.90%
				25	0.9970525	9.12995E-06		1.0054	14.605	0.00285	21.16%	21.16%
				25	0.9970525	9.12995E-06		1.0038	15.029	0.00127	16.03%	16.03%
				25	0.9970525	9.12995E-06		1.0033	15.1615	0.00064	14.43%	14.43%
				25	0.9970525	9.12995E-06		1.0017	15.5855	0.00058	9.30%	9.30%
				25	0.9970525	9.12995E-06		1.0033	15.1615	0.00064	14.43%	14.43%
				25	0.9970525	9.12995E-06		1.0017	15.5855	0.00060	9.30%	9.30%

Appendix B ERT Laboratory Test Report

Table B1: M.H Sample

Temperature (°C)	Current mA	Resistance (Ω) Cycle 1	Cycle 2	Cycle 3	Cycle 4	Average	a (m)	K	Apparent Resistivity (Ωm)	Wet soil (g)	Dry soil (g)	% WC
5	0,2	34000	34100	34100	34100	34075	0,05	0,314	10705	132,85	121,25	9,57
8	0,2	29400	30900	31000	31000	30575	0,05	0,314	9605	132,25	120,35	9,89
11	0,2	29400	29400	29400	29400	29400	0,05	0,314	9236	119,55	108,15	10,54
14	0,2	28900	28900	28900	28900	28900	0,05	0,314	9079	109,5	97	12,89
25	0,2	18600	18590	18590	18590	18592,5	0,05	0,314	5841	125,75	114,15	10,16
1st round												11
2	1	9380	9380	9380	9380	9380	0,05	0,314	2947	129,35	109,75	17,86
8	1	6540	6550	6550	6550	6547,5	0,05	0,314	2056,96	130,55	110,95	17,67
14	1	4160	4150	4150	4150	4152,5	0,05	0,314	1304,55	137,25	115,75	18,57
23	1	3990	4020	4010	4000	4005	0,05	0,314	1258,21	133,95	113,75	17,76
2nd round												18
2	1	1305	1305	1305	1305	1305	0,05	0,314	409,98	158,85	123,65	28,47
5	1	1591	1591	1592	1593	1591,75	0,05	0,314	500,06	149,95	117,05	28,11
14	1	1232	1232	1232	1232	1232	0,05	0,314	387,04	160,35	125,85	27,41
25,5	1	1242	1243	1243	1243	1242,75	0,05	0,314	390,42	151,85	119,05	28
3rd round												28
2	1	454	454	454	454	454	0,05	0,314	142,63	183,85	138,55	32,70
8	1	382	382	382	382	382	0,05	0,314	120,01	199,85	148,85	34,26
14	1	350	350	350	350	350	0,05	0,314	109,96	199,05	148,75	34
4th round												34
2	1	434	434	434	434	434	0,05	0,314	136,35	220,15	159,15	38,33
8	1	365	365	365	365	365	0,05	0,314	114,67	216,95	150,85	43,82
14	1	315	315	315	315	315	0,05	0,314	98,96	207,95	147,75	41
5th round												41

Table B2: O.T1 Sample

Temperature (°C)	Current mA	Resistance (Ω) Cycle 1	Cycle 2	Cycle 3	Cycle 4	Average	a (m)	K	Apparent Resistivity (Ωm)	Wet soil (g)	Dry soil (g)	% WC
5	0,2	2430	2430	2430	2430	2430	0,05	0,314159	763,41	147,3	131,7	11,85
8	0,2	2500	2510	2500	2500	2502,5	0,05	0,314159	786,18	144,8	129,4	11,90
11	0,2	2650	2650	2650	2640	2647,5	0,05	0,314159	831,74	139	123,1	12,92
14	0,5	1848	1848	1846	1845	1846,75	0,05	0,314159	580,17	129,25	113,85	13,53
25	0,5	2090	2110	2120	2120	2110	0,05	0,314159	662,88	144,3	129,1	11,77
1st round												12
2	1	1384	1384	1385	1385	1384,5	0,05	0,314159	434,95	146,3	125,8	16,30
8	1	1704	1691	1691	1691	1694,25	0,05	0,314159	532,26	138	119,8	15,19
14	10	545	545	545	545	545	0,05	0,314159	171,22	148,5	126,6	17,30
23	1	429	430	430	431	430	0,05	0,314159	135,09	144	123,8	16,32
2nd round												16
2	1	403	402	402	402	402,25	0,05	0,314159	126,37	156,3	129,2	20,98
5	1	501	501	501	501	501	0,05	0,314159	157,39	152,6	125,9	21,21
14	1	294	294	294	294	294	0,05	0,314159	92,36	145,4	120,9	20,26
25,5	1	292	291	291	291	291,25	0,05	0,314159	91,50	150,4	124,6	20,71
3rd round												21
2	1	181,5	181,5	181,5	181,5	181,5	0,05	0,314159	57,02	170	135,2	25,74
8	1	126,6	126,6	126,6	126,6	126,6	0,05	0,314159	39,77	183,2	147	24,63
14	1	130,5	130,5	130,5	130,5	130,5	0,05	0,314159	41,00	175,4	138,9	26,28
4th round												26
2	1	81,9	81,9	81,9	81,9	81,9	0,05	0,314159	25,73	217,5	164,7	32,06
8	1	68,6	68,6	68,6	68,6	68,6	0,05	0,314159	21,55	219,8	167,7	31,07
14	1	59,8	59,8	59,8	59,8	59,8	0,05	0,314159	18,79	211,1	160,8	31,28
5th round												31
2	1	84,6	84,6	84,6	84,6	84,6	0,05	0,314159	26,58	204,7	151,9	34,76
8	1	67,3	67,4	67,4	67,4	67,375	0,05	0,314159	21,17	189,7	137,5	37,96
14	1	58,5	58,5	58,5	58,5	58,5	0,05	0,314159	18,38	198,9	142,5	39,58
6th round												37

Table B3: O.T2 Sample

Temperature (°C)	Current mA	Resistance (Ω)					a (m)	K	Apparent Resistivity (Ωm)	Wet soil (g)	Dry soil (g)	% WC
		Cycle 1	Cycle 2	Cycle 3	Cycle 4	Average						
5	0,2	5180	5180	5180	5180	5180	0,05	0,314159	1627,34	164,87	151,37	6,63
8	0,2	5470	5450	5470	5470	5465	0,05	0,314159	1716,88	162,57	148,57	6,97
11	0,2	5250	5250	5260	5260	5255	0,05	0,314159	1650,91	151,27	137,07	7,50
14	0,2	4650	4650	4650	4650	4650	0,05	0,314159	1460,84	138,37	125,17	7,44
25	0,2	2930	2970	2990	3020	2977,5	0,05	0,314159	935,41	158,47	145,37	6,63
					1st round							7
2	1	2640	2640	2640	2640	2640	0,05	0,314159	829,38	170,67	149,67	10,40
8	1	2460	2470	2470	2470	2467,5	0,05	0,314159	775,19	169,87	149,57	10,05
14	1	709	709	709	709	709	0,05	0,314159	222,74	169,87	148,47	10,66
23	1	494	494	494	494	494	0,05	0,314159	155,19	165,67	145,17	10,38
					2nd round							10
2	1	785	795	794	794	792	0,05	0,314159	248,81	196,57	166,77	17,87
5	1	625	625	625	625	625	0,05	0,314159	196,35	188,07	160,67	17,05
14	1	582	582	582	582	582	0,05	0,314159	182,84	194,27	167,47	16,00
25,5	1	527	526	526	526	526,25	0,05	0,314159	165,33	199,07	170,57	16,71
					3rd round							17
2	1	311	311	311	311	311	0,05	0,314159	97,70	242,97	200,57	21,14
8	1	257	257	257	257	257	0,05	0,314159	80,74	224,97	186,97	20,32
14	1	224	224	224	224	224	0,05	0,314159	70,37	224,77	186,17	20,73
					4th round							21
2	1	481	481	481	481	481	0,05	0,314159	151,11	239,87	188,97	26,94
8	1	382	382	382	382	382	0,05	0,314159	120,01	219,07	173,67	26,14
14	1	150,8	150,8	150,8	150,8	150,8	0,05	0,314159	47,38	231,07	183,77	25,74
					5th round							26
2	1	286	287	287	287	286,75	0,05	0,314159	90,09	217,97	172,97	26,02
8	1	238	238	238	238	238	0,05	0,314159	74,77	231,17	173,47	33,26
14	1	212	212	212	212	212	0,05	0,314159	66,60	227,17	170,27	33,42
					6th round							31

Table B4: O.T3 Sample

Temperature (°C)	Current mA	Resistance (Ω)					a (m)	K	Apparent Resistivity (Ωm)	Wet soil (g)	Dry soil (g)	% WC
		Cycle 1	Cycle 2	Cycle 3	Cycle 4	Average						
5	0,2	5810	5830	5830	5840	5827,5	0,05	0,314159	1830,76	157,27	146,57	7,30
8	0,2	5080	5060	5060	5060	5065	0,05	0,314159	1591,22	157,07	146,17	7,46
11	0,2	5570	5580	5590	5600	5585	0,05	0,314159	1754,58	146,07	135,17	8,06
14	0,2	4150	4190	4200	4210	4187,5	0,05	0,314159	1315,54	137,67	127,47	8,00
25	0,2	2420	2420	2420	2420	2420	0,05	0,314159	760,27	158,47	147,07	7,75
					1st round							8
2	1	1923	1923	1923	1923	1923	0,05	0,314159	604,13	155,77	138,57	12,41
8	1	1400	1400	1400	1400	1400	0,05	0,314159	439,82	153,47	136,47	12,46
14	1	623	623	623	623	623	0,05	0,314159	195,72	155,17	138,67	11,90
23	1	508	509	509	509	508,75	0,05	0,314159	159,83	151,87	135,07	12,44
					2nd round							12
2	1	406	406	406	406	406	0,05	0,314159	127,55	182,37	154,67	17,91
5	1	410	410	410	410	410	0,05	0,314159	128,81	174,97	149,07	17,37
14	1	343	343	343	343	343	0,05	0,314159	107,76	182,67	156,87	16,45
25,5	1	306	306	306	306	306	0,05	0,314159	96,13	179,67	153,67	16,92
					3rd round							17
2	1	185,6	186	186	186	185,9	0,05	0,314159	58,40	271,5	173,67	23,03
8	1	142,2	142,2	142,2	142,2	142,2	0,05	0,314159	44,67	270,5	175,67	21,06
14	1	135,3	135,3	135,3	135,3	135,3	0,05	0,314159	42,51	272,7	172,87	24,30
					4th round							23
2	1	142	142	142	142	142	0,05	0,314159	44,61	210,77	161,77	30,29
8	1	133	133	133	133	133	0,05	0,314159	41,78	195,37	150,97	29,41
14	1	95,1	95,1	95,1	95,1	95,1	0,05	0,314159	29,88	211,77	165,57	27,90
					5th round							30

Table B5: T.T1 Sample

Temperature (°C)	Current mA	Resistance (Ω)					a (m)	K	Apparent Resistivity (Ωm)	Wet soil (g)	Dry soil (g)	% WC
		Cycle 1	Cycle 2	Cycle 3	Cycle 4	Average						
5	0,2	1687	1684	1684	1685	1685	0,05	0,314159	529,36	197,92	195,12	1,44
8	0,2	1054	1101	1065	1047	1066,75	0,05	0,314159	335,13	193,32	190,52	1,47
11	0,2	1140	1140	1143	1143	1141,5	0,05	0,314159	358,61	168,92	165,72	1,93
14	0,2	1079	1080	1080	1080	1079,75	0,05	0,314159	339,21	173,32	170,22	1,82
25	0,2	940	951	949	949	947,25	0,05	0,314159	297,59	199,22	196,22	1,53
					1st round							2
2	1	1303	1303	1303	1303	1303	0,05	0,314159	409,35	190,42	183,92	3,53
8	1	1141	1142	1141	1142	1141,5	0,05	0,314159	358,61	187,52	183,62	2,12
14	1	564	564	565	565	564,5	0,05	0,314159	177,34	188,52	181,92	3,63
23	1	506	506	506	506	506	0,05	0,314159	158,96	196,72	190,22	3,42
					2nd round							3
2	1	491	491	491	491	491	0,05	0,314159	154,25	217,61	204,61	6,35
5	1	467	467	467	468	467,25	0,05	0,314159	146,79	219,82	208,12	5,62
14	1	436	437	437	437	436,75	0,05	0,314159	137,21	202,22	194,92	3,75
25,5	1	316	316	316	316	316	0,05	0,314159	99,27	204,02	194,12	5,10
					3rd round							5
2	1	431	431	431	431	431	0,05	0,314159	135,40	204,32	192,92	5,91
8	1	361	361	361	361	361	0,05	0,314159	113,41	217,62	206,22	5,53
14	1	243	243	243	243	243	0,05	0,314159	76,34	217,12	203,52	6,68
					4th round							6
2	1	244	244	244	244	244	0,05	0,314159	76,65	235,12	209,22	12,38
8	1	201	201	201	201	201	0,05	0,314159	63,15	232,02	209,92	10,53
14	1	136,8	136,8	136,8	136,8	136,8	0,05	0,314159	42,98	234,82	209,12	12,29
					5th round							12

Table B6: T.T2 Sample

Temperature (°C)	Current mA	Resistance (Ω)					a (m)	K	Apparent Resistivity (Ωm)	Wet soil (g)	Dry soil (g)	% WC
		Cycle 1	Cycle 2	Cycle 3	Cycle 4	Average						
5	0,2	2150	2150	2160	2160	2155	0,05	0,314159	677,01	202,21	197,01	2,64
8	0,2	1409	1416	1416	1416	1414,25	0,05	0,314159	444,30	204,31	198,71	2,82
11	0,2	1154	1151	1150	1150	1151,25	0,05	0,314159	361,68	178,91	173,31	3,23
14	0,2	742	747	745	743	744,25	0,05	0,314159	233,81	171,31	166,01	3,19
25	0,2	1244	1232	1225	1225	1231,5	0,05	0,314159	386,89	193,21	187,51	3,04
					1st round							3
2	1	1109	1109	1110	1110	1109,5	0,05	0,314159	348,56	194,61	187,21	3,95
8	1	891	891	892	892	891,5	0,05	0,314159	280,07	190,61	184,11	3,53
14	1	550	551	551	551	550,75	0,05	0,314159	173,02	192,21	185,01	3,89
23	1	420	421	421	421	420,75	0,05	0,314159	132,18	208,01	198,51	4,79
					2nd round							4
2	1	524	524	525	525	524,5	0,05	0,314159	164,78	195,21	185,81	5,06
5	1	555	555	555	556	555,25	0,05	0,314159	174,44	194,01	184,21	5,32
14	1	380	380	380	380	380	0,05	0,314159	119,38	217,61	207,31	4,97
25,5	1	417	417	417	417	417	0,05	0,314159	131,00	199,21	191,91	3,80
					3rd round							5
2	1	402	402	402	402	402	0,05	0,314159	126,29	214,41	202,71	5,77
8	1	347	347	347	347	347	0,05	0,314159	109,01	217,31	205,21	5,90
14	1	195,9	195,9	195,8	195,8	195,85	0,05	0,314159	61,53	230,41	212,81	8,27
					4th round							7
2	1	229	229	229	229	229	0,05	0,314159	71,94	285,8	204,61	12,80
8	1	214	214	214	214	214	0,05	0,314159	67,23	288,1	209,21	11,42
14	1	134,2	134,2	134,2	134,2	134,2	0,05	0,314159	42,16	276,9	196,71	12,81
					5th round							12